



biblio.ugent.be

The UGent Institutional Repository is the electronic archiving and dissemination platform for all UGent research publications. Ghent University has implemented a mandate stipulating that all academic publications of UGent researchers should be deposited and archived in this repository. Except for items where current copyright restrictions apply, these papers are available in Open Access.

This item is the archived peer-reviewed author-version of: Determination of a quantitative relationship between material properties, process settings and screw feeding behavior via multivariate data-analysis

Authors: Bram Bekaert, Leo Penne, Wouter Grymonpré, Bernd Van Snick, Jens Dhondt, Jan Boeckx, J. Vogeeler, Thomas De Beer, Chris Vervaet, Valérie Vanhoorne

In: International Journal of Pharmaceutics, 602, Article Number: 120603

To refer to or to cite this work, please use the citation to the published version:

Bram Bekaert, Leo Penne, Wouter Grymonpré, Bernd Van Snick, Jens Dhondt, Jan Boeckx, J. Vogeeler, Thomas De Beer, Chris Vervaet, Valérie Vanhoorne (2021) Determination of a quantitative relationship between material properties, process settings and screw feeding behavior via multivariate data-analysis

International Journal of Pharmaceutics, 602, Article Number: 120603

DOI: [10.1016/j.ijpharm.2021.120603](https://doi.org/10.1016/j.ijpharm.2021.120603)

Determination of a quantitative relationship between material properties, process settings and screw feeding behavior via multivariate data-analysis

Authors

B. Bekaert^a, L. Penne^a, W. Grymonpré^b, B. Van Snick^c, J. Dhondt^c, J. Boeckx^b, J. Vogeeler^b, T. De Beer^d, C. Vervaet^a, V. Vanhoorne^a

^aLaboratory of Pharmaceutical Technology, Department of Pharmaceutics, Ghent University, Ottergemsesteenweg 460, B-9000 Ghent, Belgium

^bFette Compacting Belgium, Schaliënhoevedreef 1 b, B-2800 Mechelen, Belgium

^cOral Solid Dosage, Drug Product Development, Discovery Product Development and Supplies, Pharmaceutical Research and Development, Division of Janssen Pharmaceutica, Johnson & Johnson, Turnhoutseweg 30, B-2340 Beerse, Belgium

^dLaboratory of Pharmaceutical Process Analytical Technology, Department of Pharmaceutical Analysis, Ghent University, Ottergemsesteenweg 460, B-9000 Ghent, Belgium

***Corresponding author:**

Institution: Laboratory of Pharmaceutical Technology

Address: Ghent University, Ottergemsesteenweg 460, B-9000, Ghent, Belgium

Tel: 0032 9 264

Fax: 0032 9 264

e-mail: valerie.vanhoorne@ugent.be

Abstract

In this study, a quantitative relationship between material properties, process settings and screw feeding responses of a high-throughput feeder was established via multivariate models (PLS). Thirteen divergent powders were selected and characterized for 44 material property descriptors. During volumetric feeder trials, the maximum feed capacity (FC_{max}), the relative standard deviation on the maximum feed capacity (RSDFC_{max}), the short term variability (STRSD) and feed capacity decay (FC_{decay}) were determined. The gravimetric feeder trials generated values for the mass flow rate variability (RSDLC), short term variability (STRSD) and refill responses (V_{refill} and RSD_{refill}). The developed PLS models elucidated that the material properties and process settings were clearly correlated to the feeding behavior. The extended volumetric feeder trials pointed out that there was a significant influence of the chosen screw type and screw speed on the feeding process. Furthermore, the process could be optimized by reducing the feeding variability through the application of optimized mass flow filters, high frequency vibrations, independent agitator control and optimized top-up systems. Overall, the models could allow the prediction of the feeding performance for a wide range of materials based on the characterization of a subset of material properties greatly reducing the number of required feeding experiments.

Chapter specific abbreviations

API	Active pharmaceutical ingredient
C_P	Caffeine anhydrous powder
DCP	Emcompress AN DC/Dicalcium phosphate
FC _{decay}	Feed capacity decay
FC _{max}	Maximum feed capacity
LIW	Loss-in-weight
MCL100	Microcelac® 100/Co-processed microcrystalline cellulose and lactose
MPT _μ	Metoprolol tartrate micronized
P _μ	Paracetamol micronized
P_DP	Paracetamol dense powder
P_Gr	Paracetamol granular
P_P	Paracetamol powder
PC	Principle component
Pgel	Pharmgel/Pregelatinized maize starch
PH101	Avicel PH-101/Microcrystalline cellulose
PLS	Partial least squares
Q ²	Prediction
R ² Y	Goodness of fit
RSD _{FCmax}	Relative standard deviation of the maximum feed capacity
RSD _{LC}	Relative standard deviation of the label claim
RSD _{refill}	Relative standard deviation of the volume added during a refill
SD100	Pearlitol 100 SD/Spray-dried mannitol
STRSD	Short term relative standard deviation
T_P	Theophylline anhydrous powder
T80	Tabletose 80/Lactose
TC2020	Twin-concave screws
TS2024	Twin-spiral screws
V _{Refill}	Average volume added during a refill

1 Introduction

Continuous manufacturing has gained an increasing interest from the pharmaceutical industry in the past couple of years (W. Engisch and Muzzio, 2015a; Van Snick et al., 2019). Switching from batch to continuous manufacturing was fueled by a lack of in-line process control, scale up issues, high labor costs and a high footprint associated with batch processing (Rogers et al., 2013; Van Snick et al., 2019). Nevertheless, uncertain regulatory requirements combined with a steep learning curve are slowing down this switch (W. Engisch and Muzzio, 2015a; Ervasti et al., 2015; Ierapetritou et al., 2016).

In continuous manufacturing, feeders are generally the first crucial step and can be seen as equivalent to the weighing step in a batch process (Simonaho et al., 2016). They supply the raw materials and are crucial to maintain the correct mass balance during the manufacturing process. Any deviations from steady state will be passed down to the following unit operations (e.g. different flow behavior, deviations in the blend composition) and can affect the final product quality (Ervasti et al., 2015; Van Snick et al., 2017b; Bostijn et al., 2019).

Loss-in-weight (LIW) feeders generally consist of a material conveying part (i.e. screws) with a hopper, a load cell and an integrated control system. The load cell measures the weight of the feeder and its contents as a function of time. Via the weight difference between two consecutive measurements, the mass flow can be calculated. Additionally, the hopper can contain an agitator at its base, which serves as a secondary conveying mechanism towards the screws (Rogers et al., 2013). Another function of this agitator is to avoid arching, bridging and ratholing in the hopper, as well as decreasing the impact of hopper fill level on density changes at the screw inlet. A LIW feeder can work in two different modes: volumetric or gravimetric. The aim of feeding in volumetric mode is to feed a constant volume of material by running the equipment at a fixed screw speed. However, changes in material density (i.e. through varying degrees in powder compression due to changes in hopper fill level) and material flow will result in a variable mass flow output when a constant screw speed is used. To adjust for such changes, the gravimetric feeding mode is preferred, where the aim is to discharge a constant mass of material by changing the screw speed when needed. (Van Snick et al., 2017a). However, during hopper refill, the feeder will switch to volumetric mode, because an accurate measurement of the weight loss is not possible when powder is simultaneously leaving and entering the feeder. (Engisch and Muzzio, 2015b).

Due to the increasing interest in continuous manufacturing and the fact that feeders are a critical step in this production method, research on this unit operation is intensifying. Engisch and Muzzio developed methods to evaluate LIW feeders both gravimetrically and volumetrically. The first (i.e. trials at constant flow rate) was used to estimate the feeding performance of a material (i.e. how stable is

the feeding process), while the latter (i.e. trials at constant screw speed) was used to estimate the feeding capacity of a material (i.e. maximum output) (Engisch and Muzzio, 2012). By using these methods they managed to detect differences in feeding performance for three free-flowing powders, which could potentially generate a predictive model for the selection of appropriate feed tooling. In a later case study (Engisch and Muzzio, 2014), gravimetric feeder trials were run for five components (3 free-flowing powders, magnesium stearate and silicon dioxide) of a pharmaceutical formulation with the goal of finding the optimal feeding configuration for each component. A study performed by Cartwright et al. (2013) also showed that there was an impact of the hopper, bridge breaker and screw design on the feeding behavior of a material. Van Snick et al. performed extensive experimental work to study the impact of material properties on the residence time in twin screw feeding equipment (Van Snick et al. (2019)). Recently, Bostijn et al. investigated the feeding behavior of different raw materials on a low-throughput feeder (Bostijn et al., 2019).

Up-till-now, published feeding studies used a limited number of raw materials and/or lack determination of quantitative relationships. Furthermore, limited research is performed to establish options to optimize the feeding process related to the refill consistency and stability, which forms a crucial aspect for a continuous process in an industrial environment. Therefore, current work aims at establishing a quantitative relationship between the feeding behavior of raw materials as a function of their raw material properties and feeder configuration (i.e. screw type, screw speed) on a high-throughput feeder. Raw material characteristics were leveraged from the extensive raw material property database developed by Van Snick et al. (2018). Thirteen pharmaceutical powders were selected from the raw material property database to have a representative range of powders commonly used in the pharmaceutical industry. Volumetric and gravimetric feeding trials were performed with the selected powders on a commercially available loss-in-weight feeder (i.e. Brabender DDSR20-HD). The raw material properties and feeder configuration were correlated both with the volumetric and gravimetric feeding responses via partial least squares (PLS) regression. Additionally, throughout this study the feeding setup and processability of a wide range of raw materials was optimized for a continuous manufacturing line.

2 Materials

An overview of the selected materials can be found in **Table 1**, including the supplier information and reference to the abbreviations used throughout this chapter.

Table 1: Overview of selected materials.

Material	Supplier	Code
Paracetamol powder	Mallinckrodt	P_P
Paracetamol dense powder	Mallinckrodt	P_DP
Paracetamol micronized	Mallinckrodt	P_μ
Paracetamol granular	Mallinckrodt	P_Gr
Caffeine anhydrous powder	Siegfried	C_P
Theophylline anhydrous powder	Siegfried	T_P
Metoprolol tartrate micronized	Utag	MPT_μ
Pearlitol 100 SD	Roquette	SD100
Emcompress AN DC	JRS	DCP
Avicel PH-101	FMC	PH101
Tabletose 80	Meggle	T80
Microcelac® 100	Meggle	MCL100
Pharmgel	Cargill	Pgel

3 Equipment

3.1 Brabender DDSR20-HD

A Brabender DDSR20-HD (Brabender Technologie GmbH & Co KG, Duisburg, Germany) was used as a stand-alone loss-in-weight feeder installed on a vibration-free table.

The DDSR20-HD consists of a screw trough installed on top of a load cell. The screw trough (2.5 L) connects a twin screw conveying unit with a 5 L straight-walled extension hopper (**Figure 1**). The twin screw conveying unit is 'open' over the full screw trough width, while having a short screw barrel (**Figure 1b**). Just above the screws at the bottom of the trough a vertical agitator is integrated, which rotates counter-clockwise to ensure forced and consistent screw flight filling as well as to prevent bridging in the hopper. An additional gear reduction is present to allow the vertical agitator and screws to rotate at a fixed speed ratio, both driven by the same servo motor (Brabender Technology, 2020). A high frequency vibrator (Fette Compacting Belgium, Mechelen, Belgium) was installed on the feeder to increase the feedability of very poorly flowing materials (i.e. P_μ and MPT_μ).

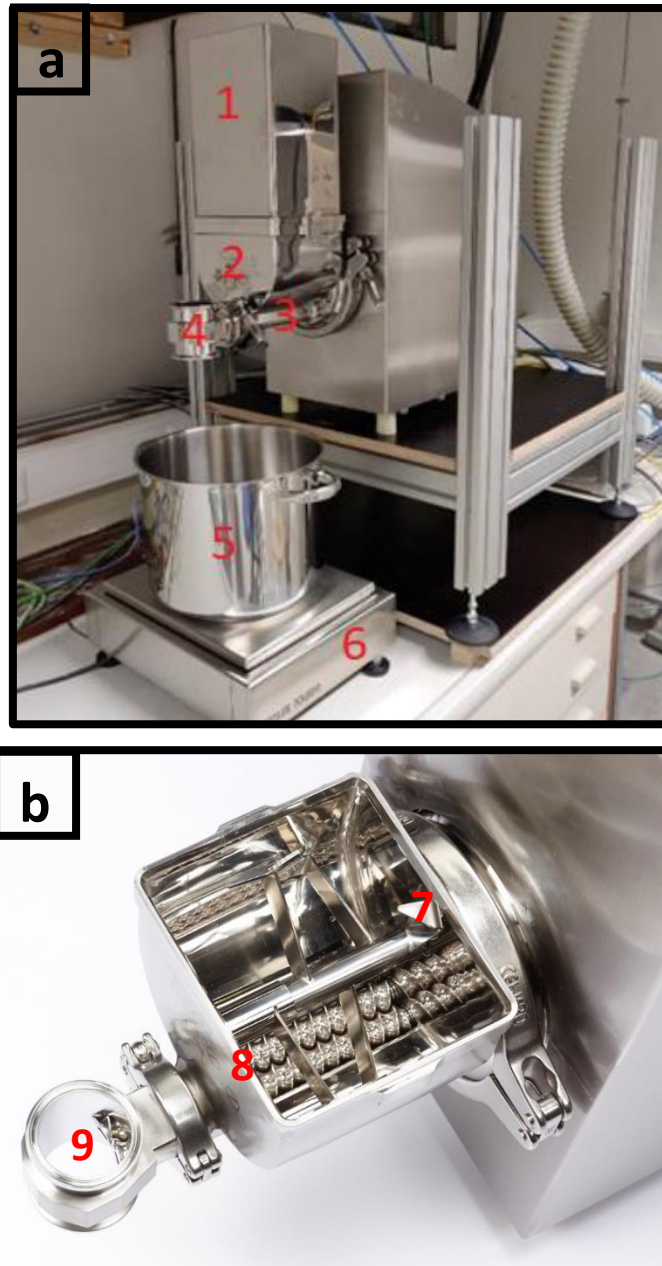


Figure 1: (a) Experimental setup for the volumetric feeder trials: (1) extension hopper; (2) screw trough with agitator; (3) screw inlet; (4) outlet; (5) charge-free metal container; (6) catch scale. (b) Inside view of the screw trough with: (7) agitator; (8) twin-concave screws; (9) outlet.

The feeder was operated using the Brabender SMART Service (version DA5.1.4.2) software and controlled using the Brabender Congrav[®] CM (Congrav[®] CM-E HW 1.0; software version 3.10) software (Brabender Technologie GmbH & Co KG, Duisburg, Germany). All feeder data (i.e. screw speed, net weight, feeding mode, hopper fill level and mass flow) was logged at 1 s intervals. The software used for the data logging (i.e. FCDA - software) was provided by Fette Compacting (Schwarzenbek, Germany).

3.2 Screw types

Three different screw types (Brabender Technologie GmbH & Co KG, Duisburg, Germany) (**Figure 2**) were used during the trials: twin-concave screws (TC2020), twin-spiral screws (TS2024) and twin-multiple flight screws. The dimensions for each screw-type can be found in **Table 2**.

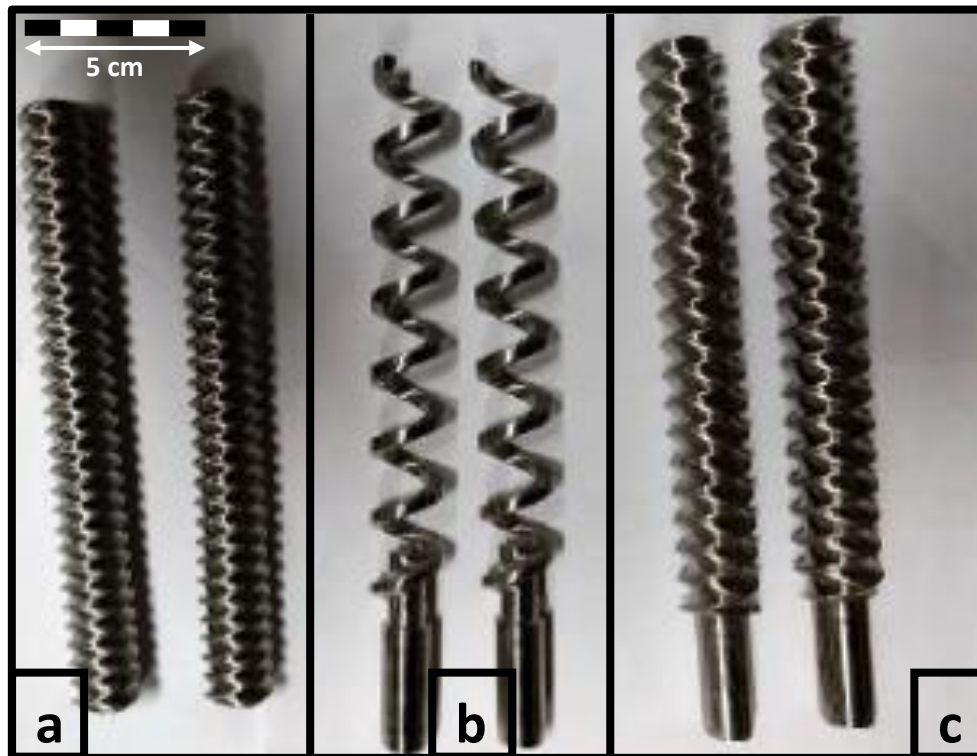


Figure 2: Different screw types used during the volumetric and gravimetric feeder trials: (a) twin-multiple flight screws; (b) twin-spiral screws; (c) twin-concave screws.

Table 2: Dimensions of the screw types.

Screw type	Length (cm)	Diameter (mm)	Pitch (mm)
Twin-concave screw (TC2020)	24	20	20
Twin-spiral screw (TS2024)	24	20	24
Twin-multiple flight screw	24	20	20

3.3 Refill system

During the gravimetric feeder trials, the feeding unit was refilled through a vacuum top-up system (**Figure 3**) consisting of a conical hopper in which pneumatic powder supply was regulated through a level sensor (Fette Compacting Belgium, Mechelen, Belgium). Hopper refill of the feeder was done through a rotating butterfly valve and materials were transported to the top-up system of the feeding unit via dilute phase vacuum conveying.

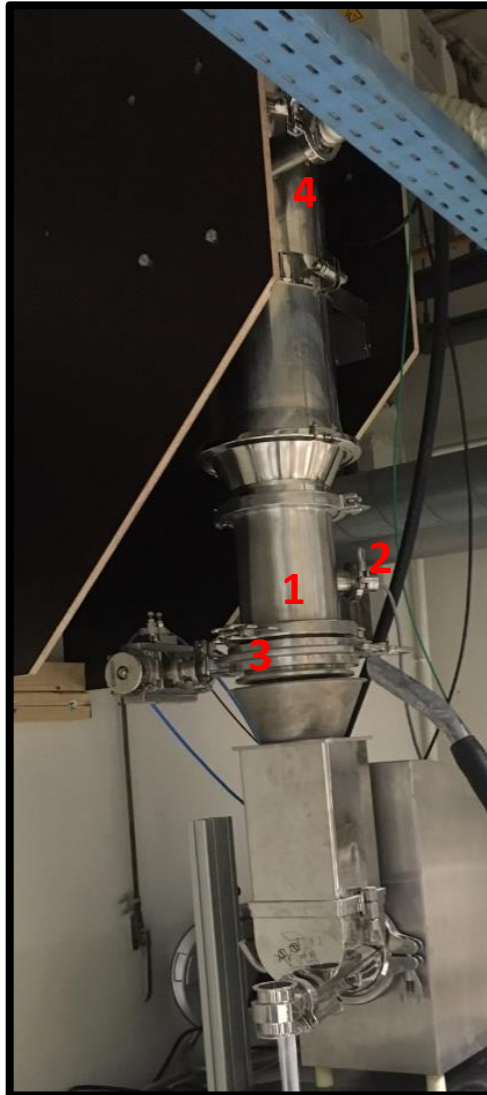


Figure 3: Vacuum top-up system consisting of: (1) a conical hopper; (2) level sensor; (3) butterfly valve; (4) dilute phase vacuum conveying.

3.4 Catch scale

A catch scale (Mettler Toledo, Zaventem, Belgium) was placed below the outlet of the feeder to record the powder feed rate at a frequency of 91.5 Hz. The powder was collected in a charge-free metal container. The catch scale data allowed to accurately monitor the ‘true’ mass flow, in contrast to the pre-filtered mass flow output of a LIW feeder.

4 Methods

4.1 Raw material selection

The selection of APIs and fillers was based on the multivariate raw material property database developed by Van Snick et al. (2018) with the aim of representing a wide range of available powders on the market. **Table 1** gives an overview of the selected materials.

4.2 Raw material characterization

Raw material characterization was performed using the protocols described by Van Snick et al. (2018) for a sub-set of material descriptors. The subset was selected based on their potential relevance during the feeding process, adopted from Van Snick B (2019). An overview of the selected descriptors, their abbreviations and applied characterization methods can be found in **Table 3**.

4.3 Feeder characterization

4.3.1 Volumetric feeder trials

The goal of the volumetric feeder trials was to characterize the inherent feeding behavior of the selected raw materials, as well as investigating the influence of different screw types and screw speeds on the process. The volumetric feeder trials were performed using a standard feeder with a default parameter list for the feeder control (PID control settings at: $P = 30$; $I = 0.5$ and $D = 0$) and the applied filter. Based on these results, the optimal screw and feeder configurations were selected for the gravimetric feeder trials.

4.3.1.1 Experimental setup

Prior to start-up, the empty feeder was tared. Next, the hopper was manually filled and the screws were primed (i.e. filling of the screws for 5 to 10 seconds) to mimic a steady state feed capacity (i.e. referred to as feed factor) at the relevant screw speed. Afterwards, the hopper was manually filled until the maximum fill level was reached. Manual refill was done in a gentle manner, preventing powder densification during filling.

Table 3: Overview of raw material descriptors and their respective abbreviation, adopted from Van Snick B (2019).

Characterization method	Descriptor	Abbreviation
Dynamic vapor sorption	Moisture content in sorption cycle at 60% relative humidity	S60
Flowpro	Flow through an orifice (= Flowrate)	FP
	Compressibility (at 15 kPa), b from Kawakita equation	C_15kPa, b
	Flow rate index, specific energy	FRI, SE
	Normalized aeration sensitivity	NAS
FT4 powder rheometer	Normalized flow energy, flow energy, residual standard deviation flow energy	nBFE, BFE, RSD_BFE
	Permeability at 1 kPa, permeability at 15 kPa	k_1kPa, k_15kPa
	Residual flowability energy (index), corresponding airflow	AE_r (AI_Er), U_r
	Susceptibility of permeability to density (slope)	k_ρ_Sus
	Wall friction angle	WFA_FT4
Granucharge	Charged density (charge-to-mass ratio)	CD
Granuheap	Drained angle of repose, cohesion	AoR_GH, sr_GH
Helium pycnometry	True density, porosity	ρtrue, ε
Laser diffraction	10, 50, 90% cumulative undersize of volumetric particle size distribution (PSD)	dv10, dv50, dv90
	Span of volumetric PSD	dspan
Loss on drying	Moisture content	LoD
Nitrogen adsorption	Specific surface area	SSA
Static image analysis	Mean aspect ratio, mean convexity, mean high sensitivity circularity, mean solidity	Armean, Cvspan, HSCLmean, Slmean
Tapping device	Bulk and tapped density	ρb, ρt
	Hausner ratio	HR
	Angle of internal friction, angle of internal friction steady state flow, effective angle of internal friction	φlin, φsf, φe
	Cohesion	τc
Ring shear tester	Consolidated density-weighted flow	ffp
	Flow function coefficient, major principal stress, unconfined yield stress	ffc, MPS, UYS
	Wall friction angle	WFA_S

After the start-up, each selected material was volumetrically fed with three screw types (i.e. TC2020, TS2024 and multiple flight screws) at six different screw speeds. Short volumetric runs were performed for the three lowest screw speeds (i.e. 5 min, 5 min and 3 min for screw speeds of 11, 55 and 99 rpm, respectively). The goal was to select the optimal screw type and to investigate the screw speed sensitivity at very low mass flows. For the higher screw speeds (i.e. 143, 187 and 432 rpm), the experiment was stopped when the feeder ran empty with the aim of generating full feed capacity profiles at the selected screw speeds. An overview of the selected screw speeds and corresponding run times can be found in **Table 4**.

Table 4: Overview of the volumetric feeder trials settings

Screw speed (rpm)	Screw speed capacity (%)	Run time
11	5	5 min
55	25	5 min
99	45	3 min
143	65	Feeder = empty
187	85	Feeder = empty
432*	90*	Feeder = empty

*A new servo motor (maximum screw speed = 480 rpm) was installed to reach higher throughputs.

By plotting the feed capacity (g/revolution) (**Eq. 1**) as a function of hopper fill level (%) (**Eq. 3**), feed capacity profiles were generated. The feed capacity was calculated from the actual mass flow (g/s) logged by the catch scale (**Eq. 2**) and screw speed (revolutions/s) logged by the feeder, using Equation (Eq.) 1:

$$\text{Feed capacity} \left(\frac{g}{\text{revolution}} \right) = \frac{\text{Mass flow} \left(\frac{g}{s} \right)}{\text{Screw speed} \left(\frac{\text{revolutions}}{s} \right)} \quad (\text{Eq. 1})$$

The actual mass flow was calculated by dividing the difference in mass ($\Delta m_{\text{catch scale}}$) (g), measured by the catch scale, by the difference in time between consecutive catch scale measurements (Δt) (s):

$$\text{Mass flow} \left(\frac{g}{s} \right) = \frac{\Delta m_{\text{catch scale}} (g)}{\Delta t (s)} \quad (\text{Eq. 2})$$

The hopper fill level was used to compare feed capacity profiles of raw materials with different densities and was calculated by normalizing the hopper net weight (g) for the maximum net weight in the hopper (g):

$$\text{Hopper fill level (\%)} = \frac{\text{Net weight (g)}}{\text{Max net weight (g)}} \times 100 \quad (\text{Eq. 3})$$

The generated feed capacity profiles were used to determine the following volumetric feeding descriptors (**Figure 4**): Maximum feed capacity (FC_{\max}), maximum feed capacity variability ($RSD_{FC_{\max}}$), short-term feed capacity variability (STRSD) and feed capacity decay (FC_{decay}).

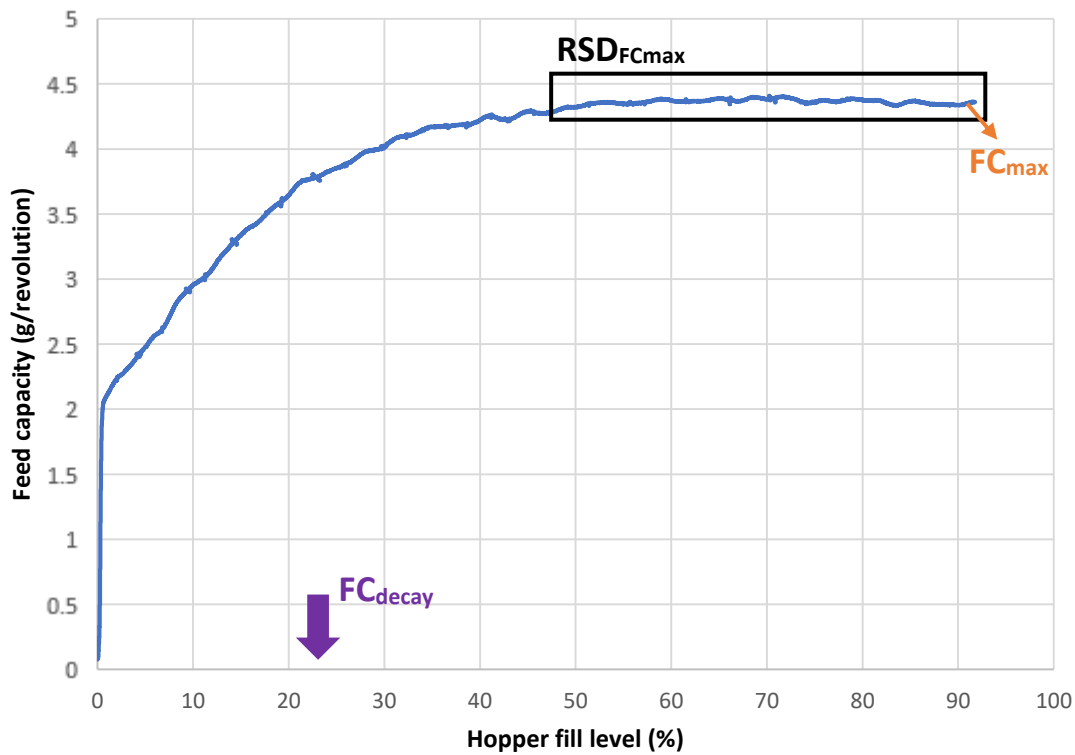


Figure 4: Feed capacity profile of theophylline anhydrous powder (T_P) at a screw capacity of 85% used to determine the volumetric feeding responses: FC_{\max} , $RSD_{FC_{\max}}$ and FC_{decay} .

4.3.1.2 Maximum feed capacity

The highest feed capacity value from the feed capacity profile was defined as the maximum feed capacity (FC_{\max}) (**Figure 4**). It correlates to the maximum feeding capacity for a specific raw material at a specific feeder configuration (i.e. screw speed and screw type).

4.3.1.3 Feed capacity variability

Most feed capacity profiles have a specific region around FC_{max} where there is no significant drift (i.e. FC variability is smaller than three times the standard deviation) in feed capacity when the hopper fill level decreases (**Figure 4**). From this region, the relative standard deviation on the maximum feed capacity ($RSD_{FC_{max}}$) was calculated according to **Eq. 4**:

$$RSD_{FC_{max}} = \frac{\text{Standard deviation (feed capacity)}}{\text{Mean (feed capacity)}} \times 100 \quad (\text{Eq. 4})$$

Another method to assess the feed capacity variability is to investigate the short-term feed capacity variability via a moving relative standard deviation. This method keeps the feed capacity profile into consideration by calculating a window of 10 consecutive measurement seconds (= equal to 1000 calculated feed capacities). The window was moved every second (= equal to 100 calculated feed capacities) across the entire feed capacity profile to generate the local relative standard deviation for every second of the feed capacity profile. Afterwards, **Equation 5** was used to calculate the mean of these local relative standard deviations.

$$STRSD (\%) = \text{mean} \left(100 \frac{\text{Local standard deviation window 1}}{\text{Mean window 1}}; \dots; 100 \frac{\text{Local standard deviation window n}}{\text{Mean window n}} \right) \quad (\text{Eq. 5})$$

4.3.1.4 Feed capacity decay

As can be seen in **Figure 4**, the feed capacity is generally maximal at 100% hopper fill level and will stay for a certain period at steady state, independent of the hopper fill level. At a certain fill level, a decrease in powder pressure typically induces a gradual decrease in feed capacity. This gradual decrease is described by FC_{decay} , which is the % hopper fill level at which the feed capacity is 90% of the FC_{max} . The FC_{decay} was used to define the refill regime during the gravimetric feeder trials in which variability introduced by a hopper refill is minimized. The threshold of 90% FC_{max} was used for refilling to ensure refilling in a stable feed capacity region, while minimizing the refill frequency (Engisch and Muzzio, 2015b; Bostijn et al., 2019).

4.3.2 Gravimetric feeder trials

Gravimetric feeder trials were performed to investigate the mass flow stability for the selected raw materials as well as the ability of the controller to reduce variability. Additionally, the influence of performing automatic refills during gravimetric runs on the steady state mass flow was evaluated.

4.3.2.1 Feeder setup

Similar to the volumetric feeder trials, the feeder was tared, the selected screws were primed and the hopper was manually filled. Next, the feeder control was internally calibrated by measuring the mass flow at a screw speed capacity of 10 and 90%. Based on the resulting feed capacities, linear interpolation will allow the control system to reach a requested mass flow faster and more accurately by initiating feeding at the estimated screw speed. Afterwards, the feeder was refilled until the hopper fill level was 100%.

For each raw material a total of five runs with increasing mass flow setpoints were performed with the aim of evaluating the mass flow variability at each setpoint. The mass flow was calculated from the actual mass flow (g/s), derived from the catch scale data (Eq. 2). At each mass flow setpoint, the ideal screw type was selected based on the results of the volumetric feeder trials. The mass flow setpoints were selected based on realistic operating ranges for fillers and APIs. An overview of the mass flow ranges and runtimes can be found in Table 5. During the gravimetric feeder runs, automatic hopper refills were initiated when the hopper fill level reached 40%. This refill level was chosen as a generally safe level, based on the results from the FC_{decay} data which ranged from 0.5 till 35%, generated during the volumetric feeder trials.

Table 5: Overview of the gravimetric trial runs for APIs and fillers.

MF setpoint API (kg/h)	MF setpoint filler (kg/h)	Screw type	Run time
0.25	1.5		30 min
0.5	4.5	Determined during	30 min
3.5	24	volumetric feeder trials	20 min
8	72	for each raw material.	15 min
56	76		10 min

4.3.2.2 Mass flow label claim

The generated mass flow profiles were used to determine if the feeder was able to reach the setpoint by calculating the average mass flow (Avg_{MF}) and the deviation from the setpoint (i.e. percentage label claim: LC) (Eq. 6) over the entire run. Based on the relative standard deviation (RSD_{LC}) (Eq. 7), the extent of variability on the mass flow rate could be quantified:

$$LC (\%) = \frac{\text{mass flow (g/s)}}{\text{mass flow set point (g/s)}} \times 100 \quad (\text{Eq. 6})$$

$$\text{RSD}_{\text{LC}} (\%) = \frac{\sqrt{\frac{\sum_{\text{h}}^1 (\text{LC} - \overline{\text{LC}})^2}{n}}}{\overline{\text{LC}}} \times 100 \quad (\text{Eq. 7})$$

with $\overline{\text{LC}}$ (kg/h) the mean label claim and n the number of time points.

4.3.2.3 Short-term mass flow variability

As previously described for the volumetric feeder trials, the short-term mass flow variability is calculated via a moving relative standard deviation with a window of 10 consecutive measurement seconds. The window was moved every 1 measurement second across the entire profile to generate the local relative standard deviation for every second. Afterwards, **Equation 5** was used to calculate the mean of these local relative standard deviations.

4.3.2.4 Gravimetric feeding disturbances

RSD_{LC} and STRSD do not provide information about the frequency of deviations in the mass flow profile, therefore, all profiles were fitted with a polynomial fit (i.e. 0 order). Next, the deviation between experimental and polynomial fit was calculated as a function of time (i.e. residual plot). From the residual plot, the duration (Res_{D}), area under the curve (Res_{AUC}) (**Eq. 8**) and amplitude (Res_{A}) (**Eq. 9**) of the rectangle with equal area under the curve were calculated, as described by Van Snick B (2019).

$$\text{Res}_{\text{AUC}} = \int_{t_{\text{start disturbance}}}^{t_{\text{end disturbance}}} \text{Residuals}(t) dt \quad (\text{Eq. 8})$$

$$\text{Res}_{\text{A}} = \frac{\text{Res}_{\text{AUC}}}{\text{Res}_{\text{D}}} \quad (\text{Eq. 9})$$

4.3.2.5 Refill

During the gravimetric feeder runs, multiple refills were performed, allowing to investigate the impact of raw material properties on this process. Refill periods were described as periods where the feeder went from gravimetric to volumetric mode. During each refill, a certain mass of powder was added to the feeder which was reflected by the increase in net weight logged by the load cells. From this increase in net weight, the total amount of material added (m_{refill}) (g) was calculated (**Eq. 10**).

$$m_{\text{refill}} (\text{g}) = \text{nw}_{\text{end of refill}} (\text{g}) - \text{nw}_{\text{start of refill}} (\text{g}) \quad (\text{Eq. 10})$$

with $\text{nw}_{\text{end of refill}}$ and $\text{nw}_{\text{start of refill}}$ the net weight at the end and start of the refill, respectively. The amount of material being discharged by the feeder during this period (i.e. up to 42 g) was insignificant compared to the total amount of material added (i.e. up to 2500g) and therefore was not taken into

account. For each selected raw material, the average volume added after each refill (V_{refill}) (g) and the variability ($\text{RSD}_{\text{refill}}$) (%) of this parameter were calculated (Eq. 11 and 12).

$$V_{\text{refill}} = \frac{\overline{m_{\text{refill}}}}{\rho_b} \quad (\text{Eq. 11})$$

$$\text{RSD}_{\text{refill}}(\%) = \sqrt{\frac{\sum_{h=1}^n (\overline{m_{\text{refill}}} - m_{\text{refill}})^2}{n}}{\overline{m_{\text{refill}}}} \times 100 \quad (\text{Eq. 12})$$

with $\overline{m_{\text{refill}}}$ the average mass added after a refill, n the number of time points and ρ_b the bulk density of the raw material. Additionally, the refill system was visually inspected to check for potential problems (e.g. material adhering to the walls, vacuum conveying problems,...).

4.3.3 Multivariate data analysis

For both the volumetric and gravimetric feeder trials PLS models were developed. These models regressed the raw material properties and process parameters (X-matrix) versus the feeding responses (Y) of the 13 selected materials. Separate PLS models were created and optimized for each of the described feeding responses to increase the goodness of fit (R^2) and predictive ability (Q^2). Descriptors with no significant correlation were removed from the models if their removal had a significant impact on the R^2 and Q^2 . In the volumetric PLS models, the tested screw speeds and screw type were included as process parameters in the X-matrix. Similarly, the different mass flow setpoints were added to the X-matrix of the gravimetric PLS models. The datasets for all models were pre-treated prior to PLS regression via unit variance (UV) scaling and mean-centering. Finally, log transformation was applied to non-normally distributed responses. The PLS models were created using the SIMCA software (Version 16, Umetrics, Umeå, Sweden).

5 Results and discussion

5.1 Raw material selection

First a selection of representative and challenging APIs and fillers was made based on the raw material database described by Van Snick et al. (2018).

5.1.1 API selection

Due to the high importance of accurate and precise API feeding, seven APIs with different material properties were selected aiming to cover a wide variety of APIs. The selection was performed using a multivariate approach, considering the influences of all the measured properties (**Figure 5a**).

The first step was to select raw materials at the edges of the API cluster: paracetamol granular (P_Gr) was chosen mainly for its granular nature and high density; theophylline anhydrous powder (T_P) as a semi-cohesive model API and metoprolol micronized (MPT_μ) for its micronized state and triboelectric charging. Next, three additional paracetamol grades were selected to investigate the influence of different material grades. Paracetamol powder (P_P) was chosen as an intermediate grade, paracetamol dense powder (P_DP) as the high density grade and paracetamol micronized (P_μ) as a highly cohesive and micronized active component. Finally, caffeine anhydrous powder (C_P) was included as an API with intermediate properties compared to the other APIs.

5.1.2 Filler selection

Six fillers, commonly used in wet granulation or direct compression were selected, using a multivariate approach, considering the influences of all the measured properties (**Figure 5b**).

First, fillers at the edges of the filler cluster were chosen: Avicel PH-101 (PH101) as a cohesive and highly compressible component; Emcompress AN DC (DCP) due to its high density and flowability; Microcelac 100 (MCL100) as a good flowing model filler and Pharmgel (Pgel) with a high wall friction. Next, Pearlitol 100SD (SD100), which was located close to MCL100, was picked to confirm that other good flowing fillers in the same region behave in a similar fashion. Finally, Tablettose 80 (T80) was included as a filler with intermediate properties compared to the other fillers.

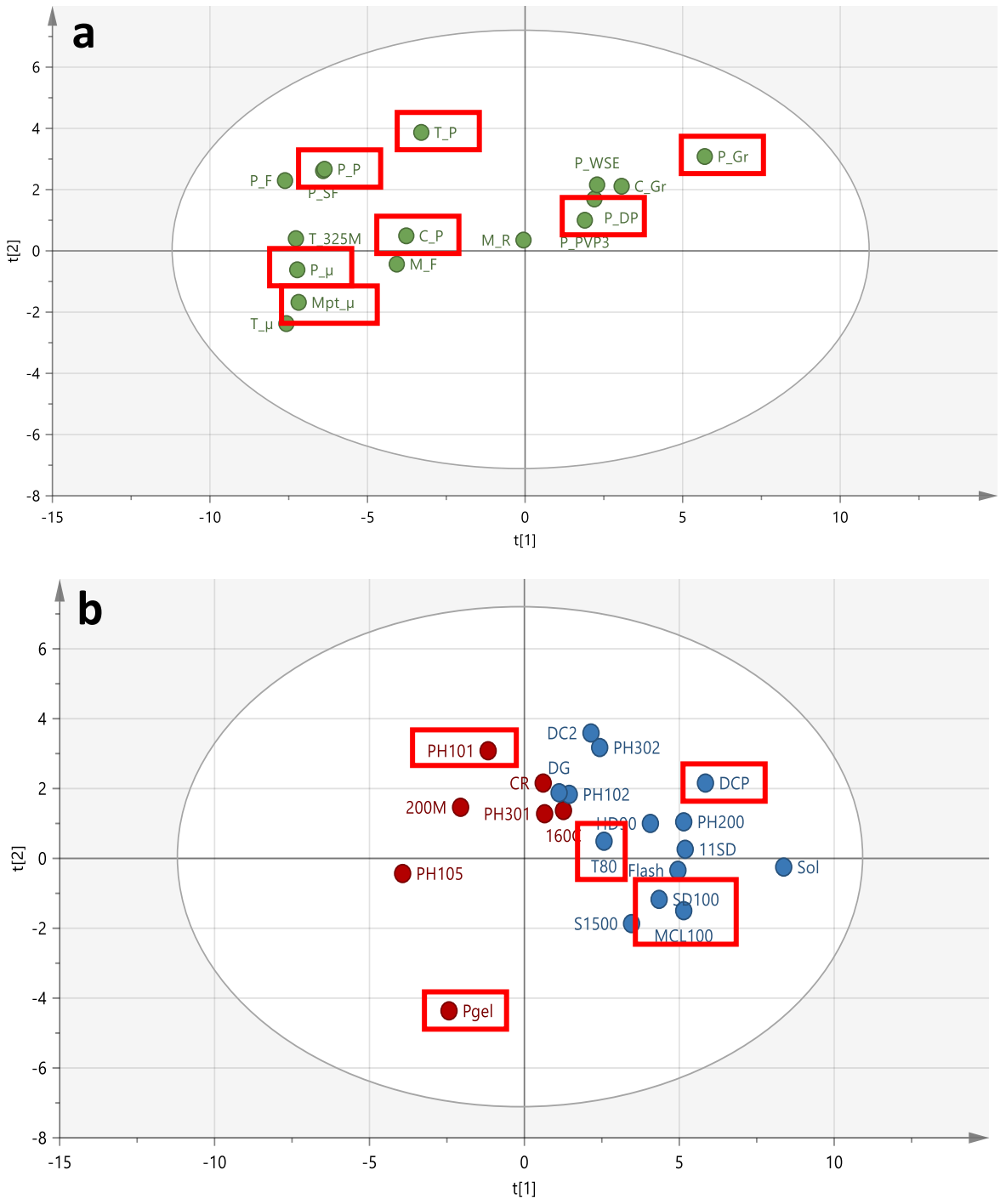


Figure 5: PLSC 1 vs 2 scores for (a) the API and (b) filler cluster, adapted from Van Snick et al. (2018).

5.2 Optimization of the feeding process

During the volumetric and gravimetric feeder trials, the experiments and experimental setup revealed some challenges that could happen during tests in an industrial environment. Therefore, an overview of the occurring challenges and potential solutions are outlined below.

During the volumetric feeder trials, the internal filtering of the Brabender DDSR20-HD resulted in pre-treated mass flow profiles where essential information was not visible. As commonly seen with feeders (Engisch and Muzzio, 2012), the internal filtering could result in data shown by **Figure 6** where the data for a specific trial run generated by both the feeder loadcell (pre-treated data) and the catch scale (raw data) is shown. The catch scale data (i.e. **Figure 6a**) displayed a significant and important deviation at the start of the run (see the red circle) which was not visible in the filtered loadcell data when using the default parameter set. These observations were seen for all performed volumetric trial runs and indicated that it is essential to use less filtered mass flow signals. Changing the filter parameters resulted in more representative mass flow profiles. The new filter settings were then used for the gravimetric feeder trials.

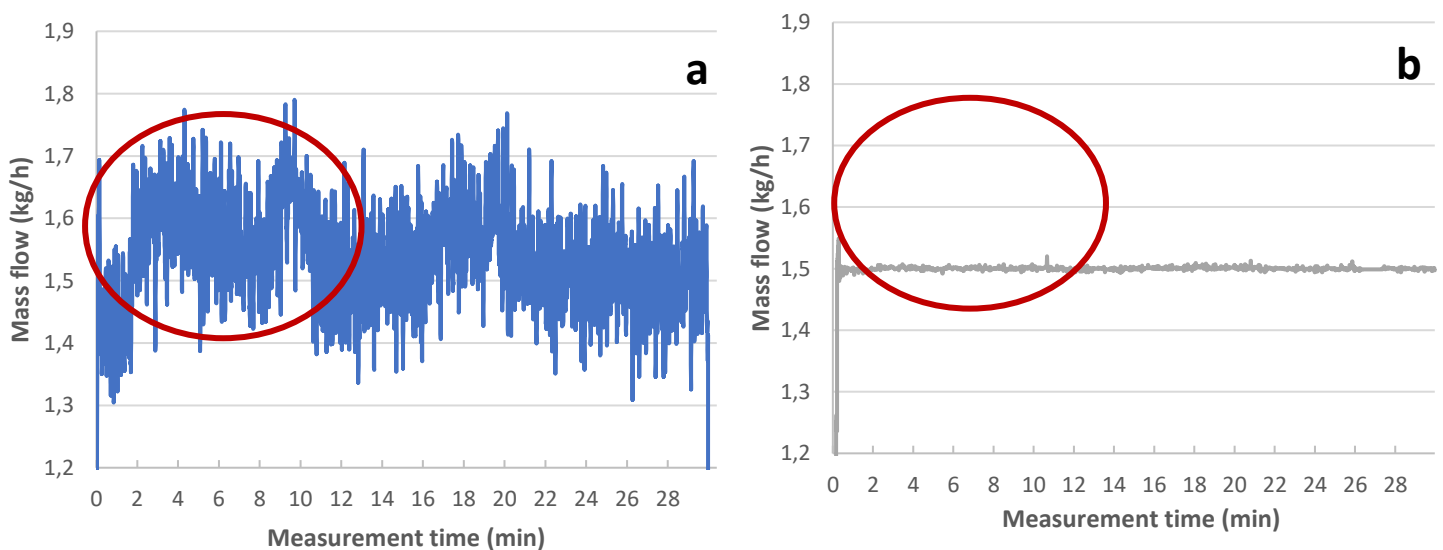


Figure 6: Mass flow profiles for PH101 at a throughput of 1.5 kg/h with twin-concave screws generated via (a) a catch scale and (b) the default parameter set for the feeder load cell. The red circle indicates there was a significant deviation introduced by the feeder.

A second and often re-occurring problem when feeding cohesive materials is their adhesion to the hopper wall and the formation of ratholes or bridges (**Figure 7**). **Figure 8** depicts the feed capacity profile of a volumetric run with paracetamol micronized, a raw material that has a high tendency to form bridges or ratholes. The profile shows an abnormal decrease in feed capacity until the recovery at around 80% hopper fill level. These drops in feed capacity or mass flow are caused by the incomplete screw filling of the feeder. Not achieving the expected feed capacity or mass flow is a typical example

of bridging or ratholing behavior. This could be solved by the application of a high frequency vibrator on the hopper. In most cases low frequency vibrations were sufficient to resolve the problem, but during these trials the problems remained for the very cohesive P_{μ} and MPT_{μ} . Therefore, high frequency vibrations were applied to the feeder and hopper to reduce the friction of the powders to the wall (Dunst et al. (2018)). To investigate this effect, volumetric runs performed with P_{μ} and MPT_{μ} were repeated with the addition of a high frequency vibrator. The positive effect can be seen in **Figure 8**, compared to the same volumetric run previously performed. In addition to the reduction in bridge or rathole formation, the increased flowability of the powder resulted in a higher FC_{max} as well as a lower variability ($RSD_{FC_{max}}$ and $STRSD$). The repeated runs with high frequency vibrations for P_{μ} and MPT_{μ} were included into the final volumetric and gravimetric feeding models.



Figure 7: Rathole formation during a volumetric run with paracetamol micronized (P_{μ}).

5.3 Volumetric feeder trials

5.3.1 Feed capacity profile characterization

The feed capacity profiles showed a decrease in feed capacity variability with increasing screw speeds. This behavior was present for all selected materials in different degrees (illustrated in **Figure 9** for a filler and API), which suggests an impact of the material properties. **Figure 9** depicts the feed capacity profiles of Microcelac 100 and theophylline generated with twin-concave screws at the lower screw speeds (i.e. 11, 55 and 99 rpm).

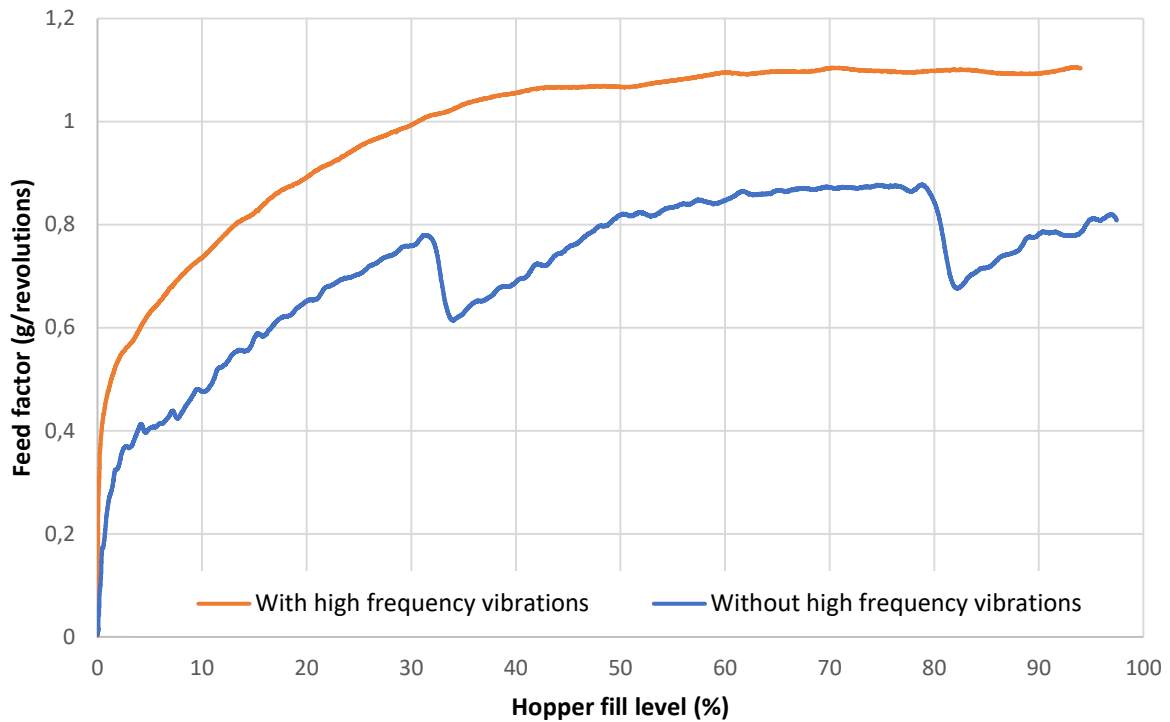


Figure 8: Irregular feed capacity profile of paracetamol micronized (P_{μ}) at a screw speed of 187 rpm with twin-concave screws (blue line) and the feed capacity profile of P_{μ} with the application of high frequency vibrations (orange line).

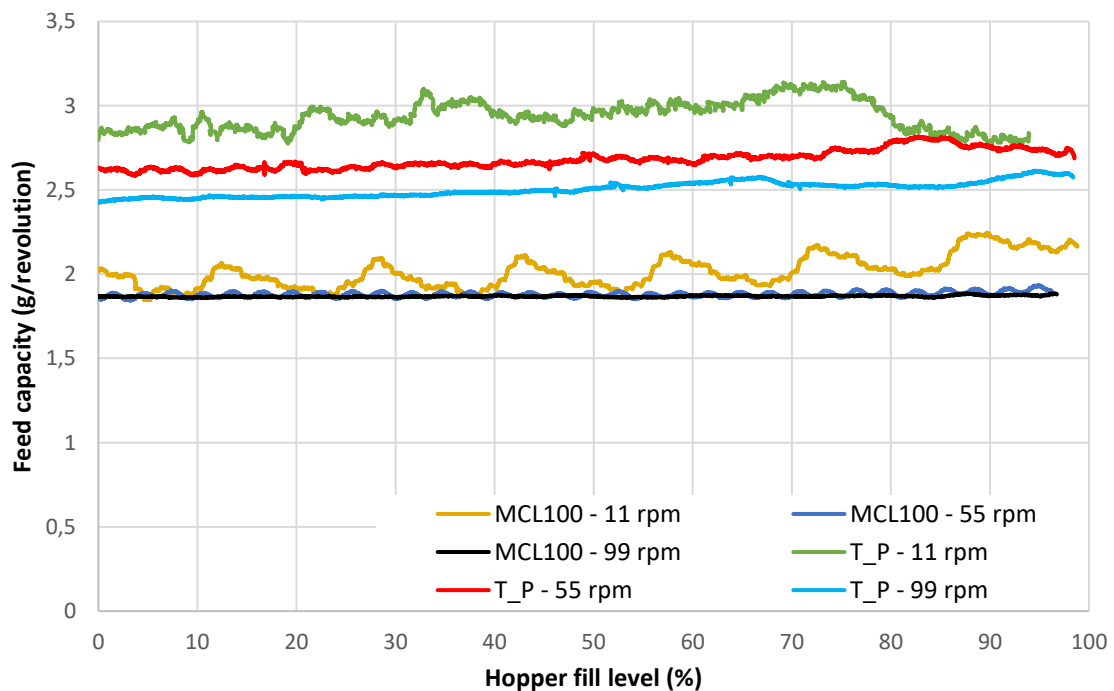


Figure 9: Feed capacity profiles of Microcelac®100 (MCL100) and theophylline anhydrous powder (T_P) at screw speeds of 11, 55 and 99 rpm with twin-concave screws used to investigate the screw speed sensitivity.

Additionally, **Figure 9** shows a cyclic behavior of the feed capacity which was attributed to the speed of the agitator in the hopper. Each time a blade from the agitator pushes the powder downwards into the screws, an increase in feed capacity can be seen due to the corresponding forced screw filling, which was more pronounced for materials with a higher density (e.g. MCL100). This phenomenon is more frequent at higher screw speeds since both the screws and agitator are controlled by the same servo motor. However, a higher agitator speed reduces the forced screw filling time, thus reducing the degree of feed capacity increase with every agitator blade pass. Furthermore, it was observed that at low screw speeds the vertical agitator increased the risk of bridge formation by pushing the powder upwards and giving the powder time to densify and form these bridges. At higher screw speeds there was insufficient time for the upward pushed powder to densify, thus reducing the potential of bridge formation. These observations suggested that a separate drive which controls the agitator speed independently from the screw speed, could be helpful in reducing the observed problems.

For most of the selected materials, the gradual decay in feed capacity occurred faster (e.g. around 35% and 45% hopper fill level for MPT_μ and T_P, respectively) compared to volumetric runs where the decay started when the hopper was almost empty (i.e. observed for P_{GR}, MCL100, T80 and SD100)(**Figure 10**). The difference in onset of decay was attributed to the very good flowability of the latter materials, resulting in consistent screw filling even when the pressure from the powder in the hopper is removed. It can also be noted that the poor flowability and consequently inconsistent screw filling of very cohesive materials generated irregular feed capacity profiles (e.g. P_μ profile without the application of high frequency vibrations (blue line) in **Figure 8**). Additionally, the cohesive materials are more prone to generate bridges and ratholes in the hopper, impeding consistent screw filling.

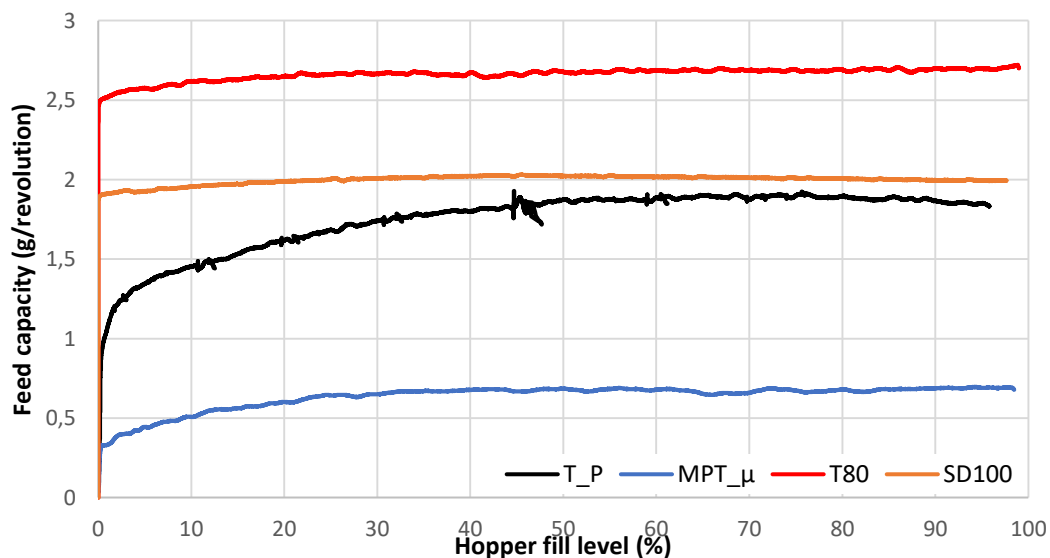


Figure 10: Feed capacity profiles of theophylline anhydrous powder (T_P), metoprolol tartrate micronized (MPT_μ), Pearlitol 100SD (SD100) and Tablettose 80 (T80) at a screw speed of 187 rpm with twin-concave screws used to illustrate the different degrees in feed capacity decay.

5.3.2 Partial least squares regression modeling

Table 6 displays an overview of the constructed PLS models with their corresponding goodness of fit (R^2Y), prediction (Q^2) and number of principle components (#PC). The corresponding scores and loadings plots elucidated correlations between the material properties, process settings and selected feeder response (i.e. FC_{max} , $RSD_{FC_{max}}$, FC_{decay} and STRSD). The scores plot shows the relationship of the selected powders to each other based on their properties and feeding behavior. The loadings plot reveals the correlations between material properties and their impact on the feeding responses. Both the scores and loadings plot are superimposable, which means that materials with a specific location on the scores plot have high values for the variables (i.e. material properties and feeding responses) on the same location in the loadings plot and low values for those at the opposite side of the origin. Additionally, coefficients plots were used to get better insight into the correlations. Positive values for a descriptor in a coefficient plot indicate a positive correlation between that descriptor and the feeder response. The significance of these values was determined using a 90% confidence level.

Table 6: Overview of the constructed PLS models for the volumetric feeder trials. R^2Y and Q^2 is given for each sub model and each principle component.

Model	R^2Y	Q^2	#PC
FC_{max}	0.906	0.901	3
↳ PC1	0.411	0.406	
↳ PC2	0.790	0.784	
↳ PC3	0.906	0.901	
$RSD_{FC_{max}}/STRSD$	0.681	0.586	3
↳ PC1	0.210	0.188	
↳ PC2	0.595	0.496	
↳ PC3	0.681	0.586	
FC_{decay}	0.645	0.600	2
↳ PC1	0.579	0.566	
↳ PC2	0.645	0.600	

5.3.2.1 Maximum feed capacity

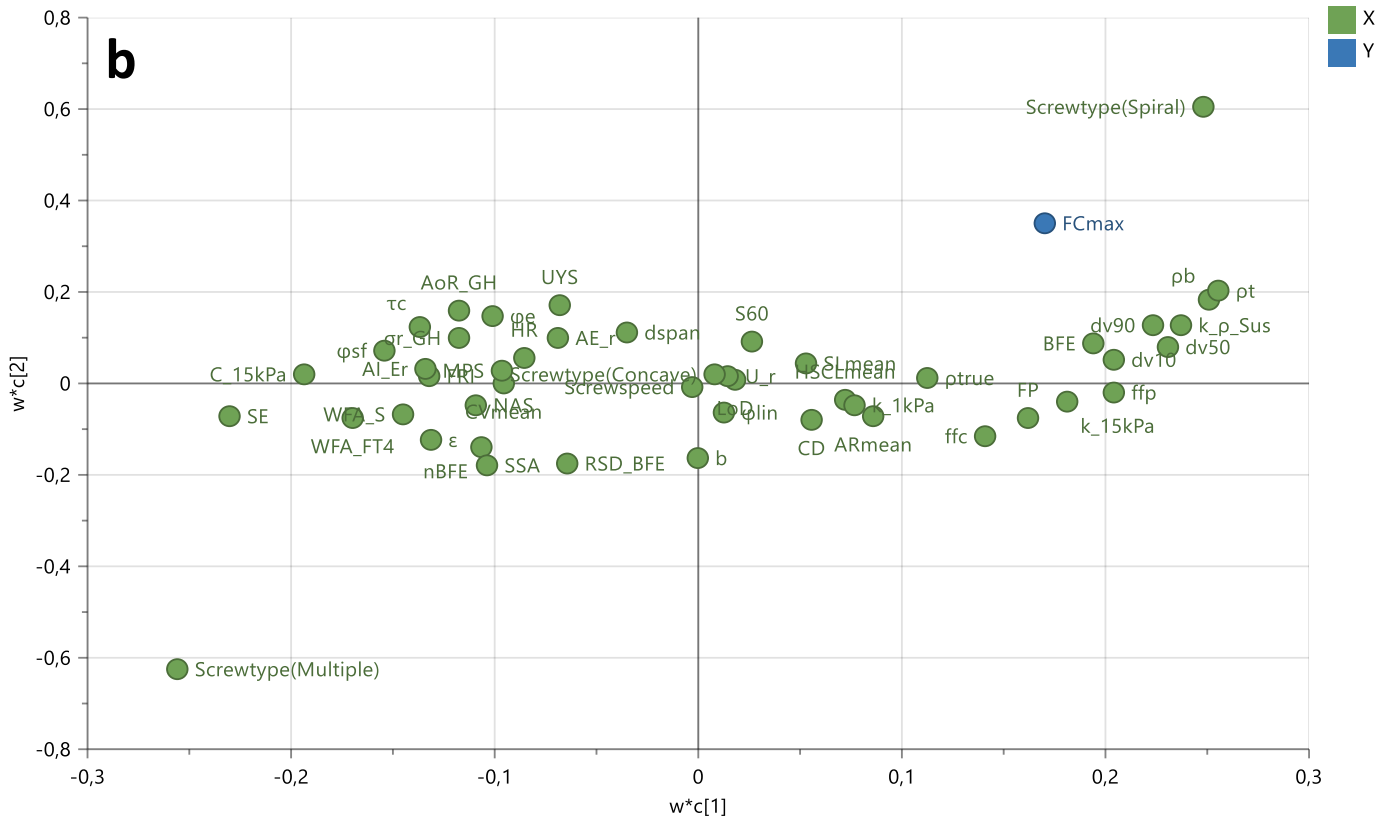
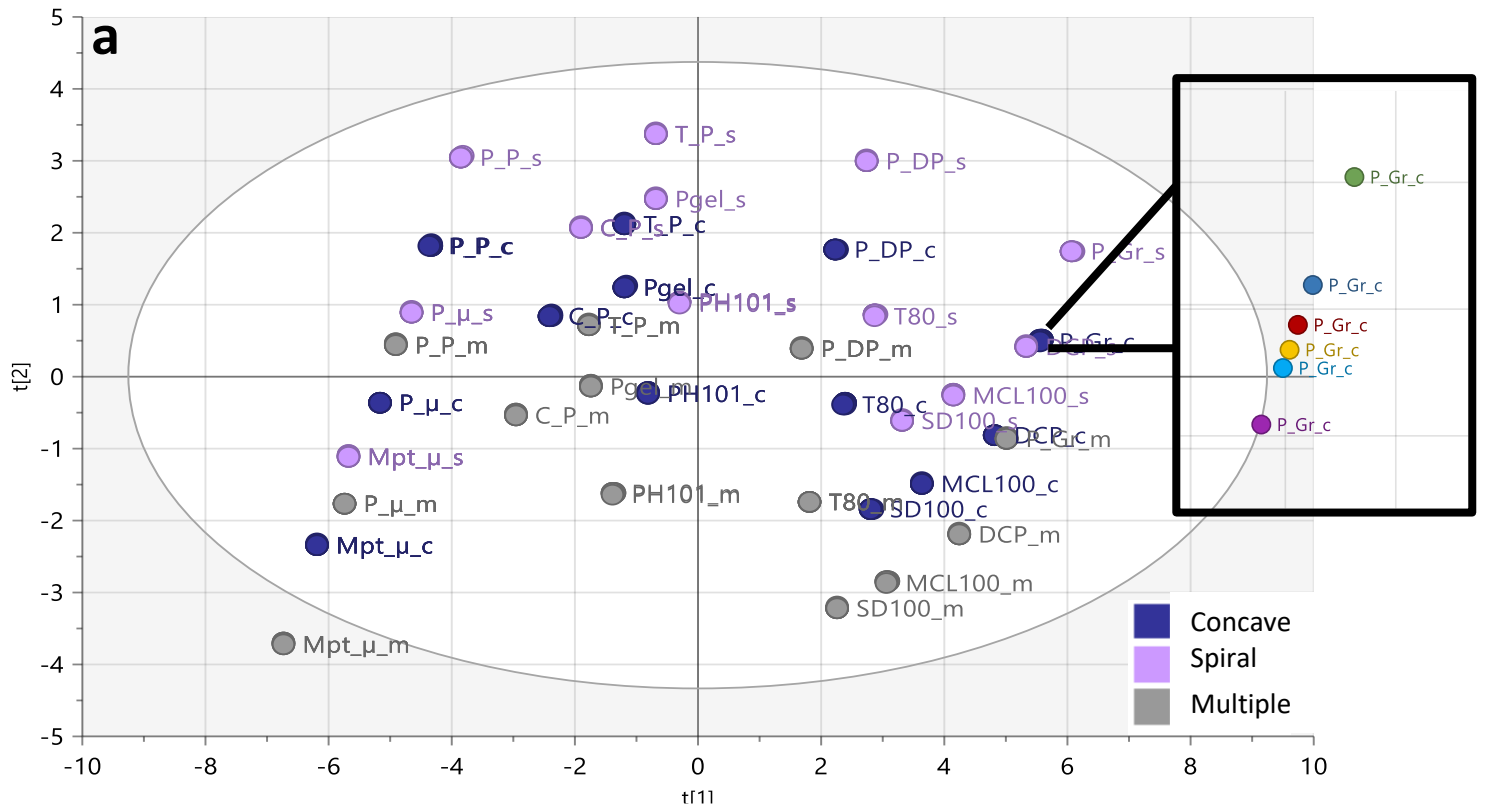
A three-component PLS model was developed for FC_{max} which explained 90.6% of the variation in the Y-matrix (**Table 6**). **Figure 11** depicts the scores and loadings plots for PC1 vs PC2. Whereas PC1 is determined by the raw material properties, PC2 has the screw type as its main descriptor. Additionally, the screw speed was located close to the origin of the loadings plot indicating that there is no correlation with FC_{max} . The third principle component (i.e. PC3)(**Figure 11c**) could not be attributed to

a specific descriptor, however it was retained in the model due to the significant increase in the goodness of fit (R^2Y) and prediction (Q^2) from 0.790 to 0.906 and 0.784 to 0.901, respectively.

The loading plot for PC1 vs PC2 indicates that FC_{max} is regulated by the screw type, flowability (ffp, ffc and BFE), density of the material (ρ_b and ρ_t), as well as the compressibility (C_{15kPa}), permeability (k_{15kPa} , k_{ρ_sus}) and wall friction angle (WFA_FT4 and WFA_S). The coefficient plot (**Figure 12**) was used to investigate the significance of the correlations derived from the loadings plot. The influence of screw type can be explained by the fact that screws with a higher screw volume will be able to transport a higher volume of material per revolution, thus resulting in a higher feed capacity. Regarding the density, a higher density means that a higher amount of material can be present in the screw flight, increasing the output of material per screw revolution. In the same cluster on the loadings plot, a positive contribution to the maximum feed capacity can be found for the particle size (i.e. dv_{10} , dv_{50} and dv_{90}), density-weighted flow (ffp) and basic flowability energy (BFE). Particles with a larger particle size generally have a better flow ensuring more screw filling. The descriptor ffp is a combination of the flow function coefficient and density into one value. This descriptor and the basic flowability energy, which is another descriptor for powder flow, confirms that the combination of good flowability and a high density will ensure optimal screw filling.

Consequently, on the other side of the loadings plot there is a cluster of descriptors indicating adhesive and cohesive properties (RSD_BFE, SE, WFA_S/FT4, SSA, MPS, AoR_GH, τ_c) (**Figure 11b**) which negatively affect FC_{max} , due to inconsistent screw filling of such materials. The inverse nature of porosity (ϵ) to the density resulted in a negative impact that could be observed in the loadings and coefficient plot (**Figure 12**).

On the other hand, the multivariate approach also indicated that less used material descriptors such as permeability (k_{15kPa} , k_{ρ_sus}), compressibility (C_{15kPa}) and wall friction angle (WFA_FT4 and WFA_S) had a significant impact on FC_{max} and could be used for predictive purposes. A highly permeable material will fluidize more easily, resulting in a better screw flight filling and thus higher FC_{max} . Compressibility had a negative impact because highly compressible materials also showed a high cohesivity. Raw materials with a high wall friction angle (i.e. high tendency to adhere to a wall) showed difficulties to generate a consistent and optimal powder flow to the screws with a lower FC_{max} as a result.



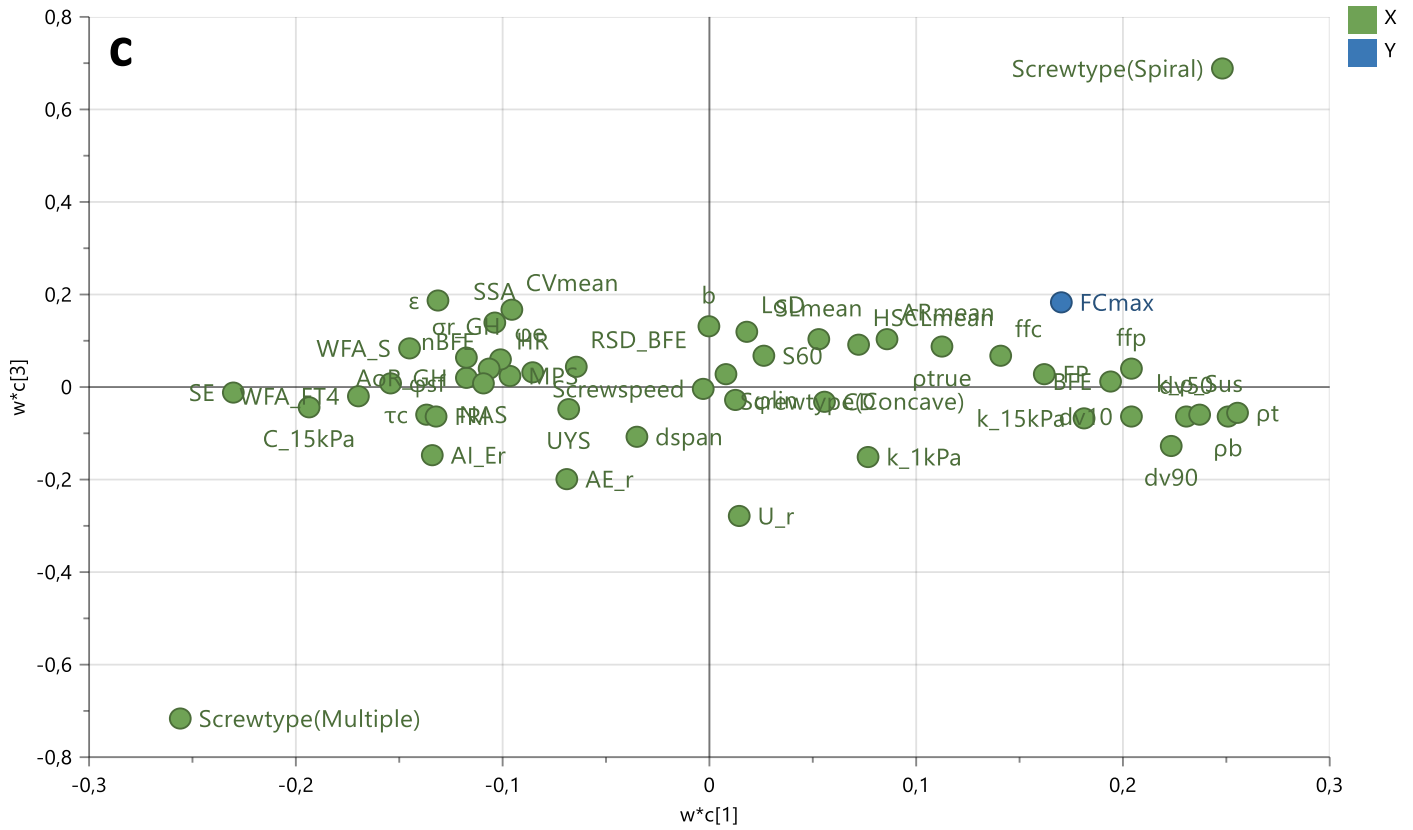


Figure 11: PC 1 vs PC 2 scores (a) and loadings (b) plot and PC 1 vs PC3 loadings plot (c) of the FC_{max} model. The naming consists of the product name followed by the screw type (i.e. $_s$ = twin-spiral screws; $_c$ = twin-concave screws; $_m$ = twin-multiple flight screws). The enhancement of one cluster shows the location of the different screw speed capacities.

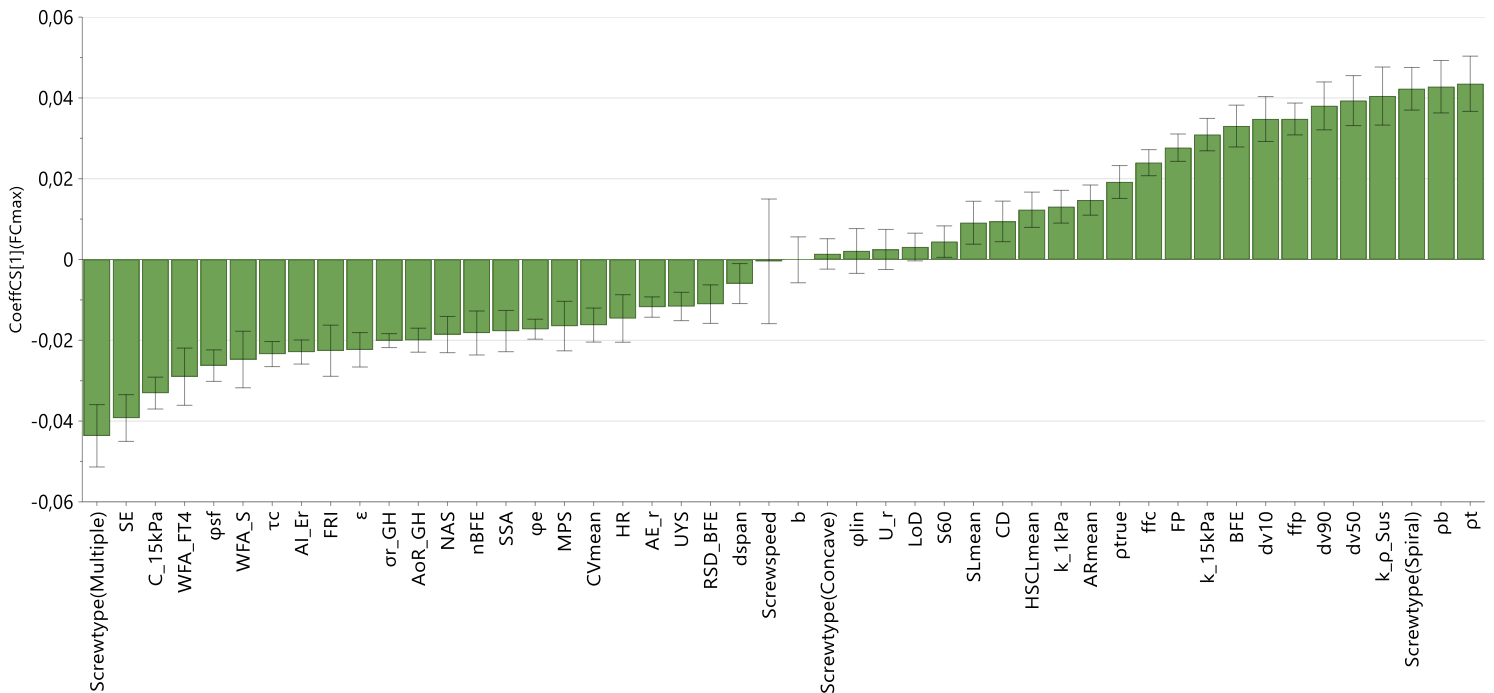


Figure 12: Coefficient plot for the FC_{max} model. Significance was determined using a 90% confidence interval.

5.3.2.2 Feed capacity variability

Two different approaches were used to describe the variability, generating one general PLS model. The model consisted of three PCs, explaining 68.1% of the variation (**Table 6**). Looking at the responses along the first principle component (x-axis), they mainly describe the material properties. Along the y-axis (= PC2) the main contributors are the process settings (i.e. screw speed and screw type), with screw speed as the largest contributor (**Figure 13**).

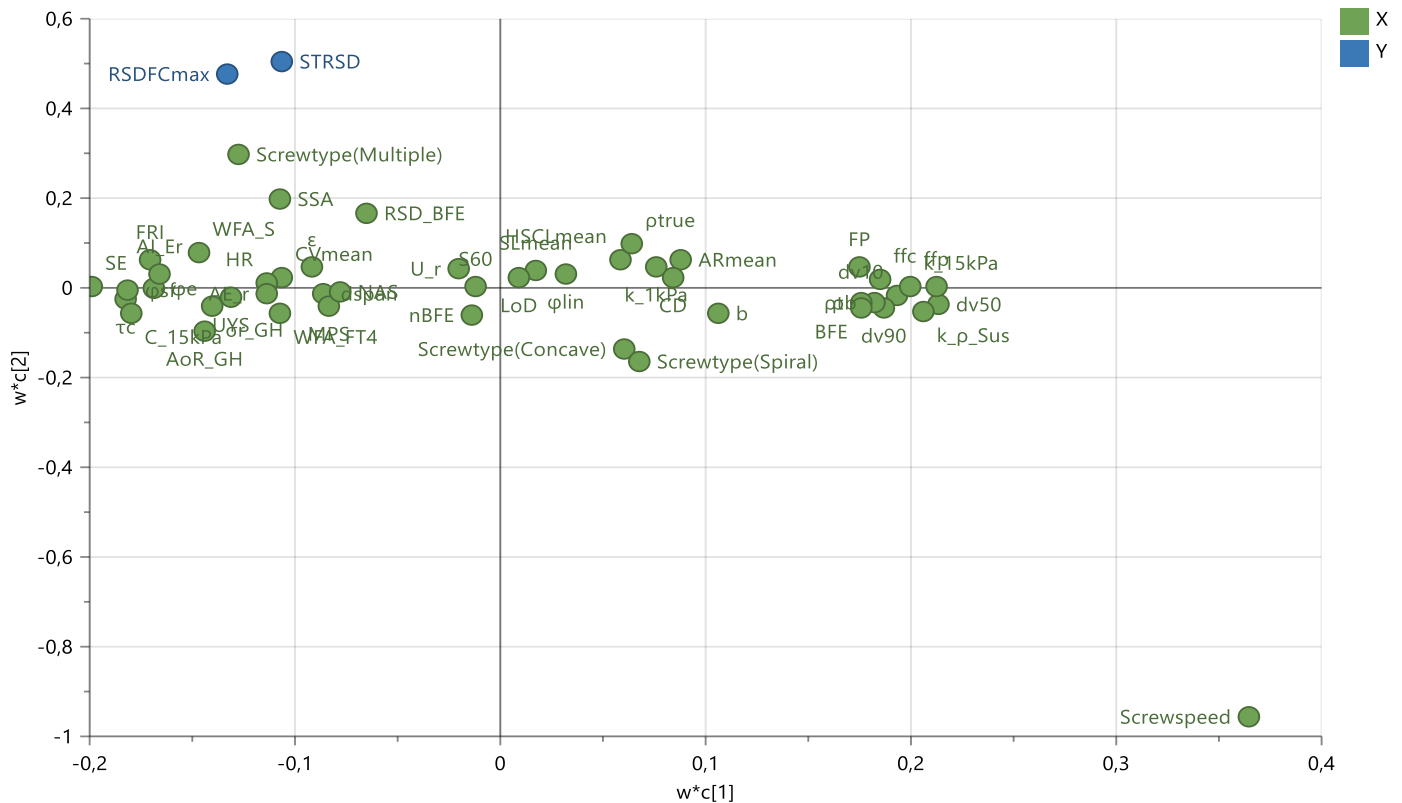


Figure 13: PC 1 vs PC 2 loadings plot of the RSD_{FCmax} and STRSD model.

It is clear that both RSD_{FCmax} and STRSD are negatively correlated to the screw speed, since they are located at opposite sides of the origin. This observation can be visualized by plotting RSD_{FCmax} and STRSD in function of the screw speed, as depicted for the latter in **Figure 14**. To avoid the high variability at the lower screw speeds, using a low-throughput feeder could be advised (Bostijn et al. (2019)). Additionally, **Figure 14** depicts a non-linear correlation between the screw speed and feed capacity variability. Looking at PC1 along the x-axis, a positive correlation can be observed between a high feed capacity variability (both STRSD and RSD_{FCmax}) and raw materials with a low density, poor flow, small particle size, high compressibility and high cohesive and adhesive properties (**Figure 13**). These properties are all related to a poor and inconsistent screw filling, thus generating a higher variability of the feed capacity.

Looking at the location of the twin-multiple flight screws (i.e. Screw type (Multiple)), there is a positive contribution to the feed capacity variability. This contribution can be attributed to the low screw flight volume, which can impede consistent screw filling. The reduced volume will make it difficult for materials with low flowability to accurately and consistently fill the screws, thus increasing the variability in feed capacity. The other two screw types are located around the origin, thus having a limited contribution. In this case, the material properties or screw speed are the dominating variables that need to be taken into consideration.

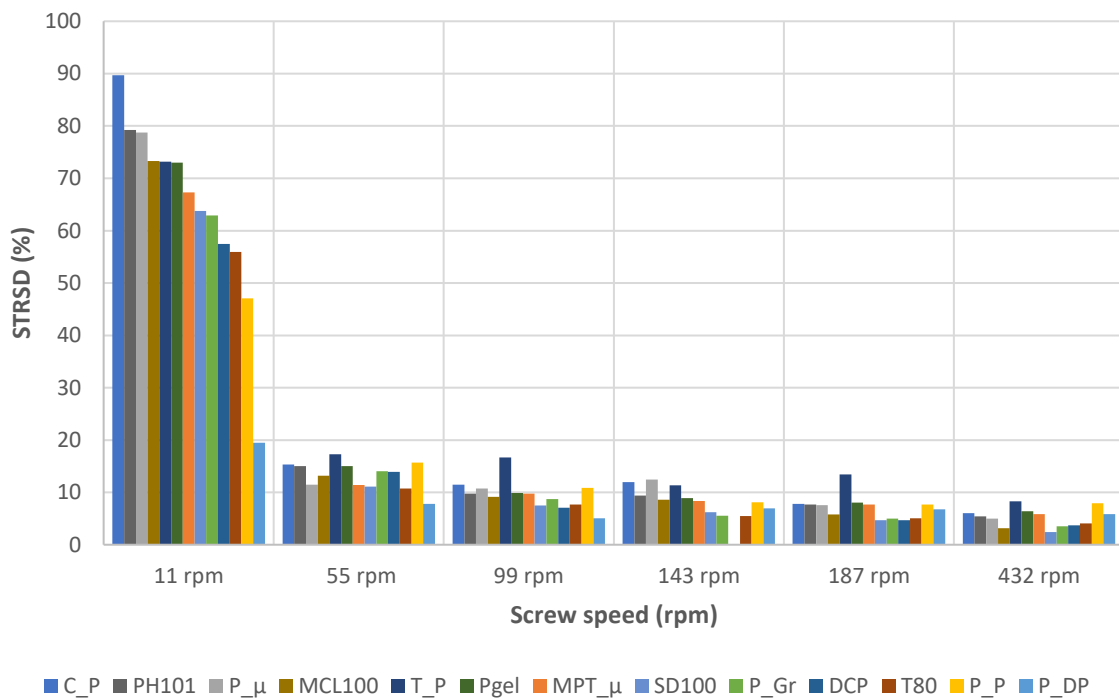


Figure 14: STRSD in function of the screw speed for the twin-concave screws demonstrating a non-linear correlation. A similar correlation between STRSD and SS was found for the twin-spiral and twin-multiple flight screws.

5.3.2.3 Feed capacity decay

The influence of material properties and process settings on the decay (FC_{decay}) was investigated via a PLS model with two components, explaining 64.5% of the variation (**Table 6**). In this model, PC1 explained 57.9% of the variation along the x-axis with the material properties as the main contributors.

Closely located to FC_{decay} is a descriptor for compressibility of the powder bed (i.e. C_{15kPa}) (**Figure 15**), indicating a positive correlation. This correlation can be explained by the fact that at 100% hopper fill level (i.e. high powder mass in the hopper) the powder at the screw inlet will be compressed to its maximum density resulting in the highest feed capacity. As the powder level in the feeder drops, the lower amount of material will apply less pressure, thus decreasing the density of powder at the

screw inlet and generating a lower feed capacity. Materials that have a high compressibility (e.g. Pgel, P_μ) are more susceptible to these compressive forces, resulting in a faster reduction of the feed capacity (= high FC_{decay}) when the hopper runs empty. For materials with a low compressibility there is a minimal impact of these compressive forces on the density at the screw inlet, therefore an almost constant feed capacity can be seen when the hopper runs empty (**Figure 10**).

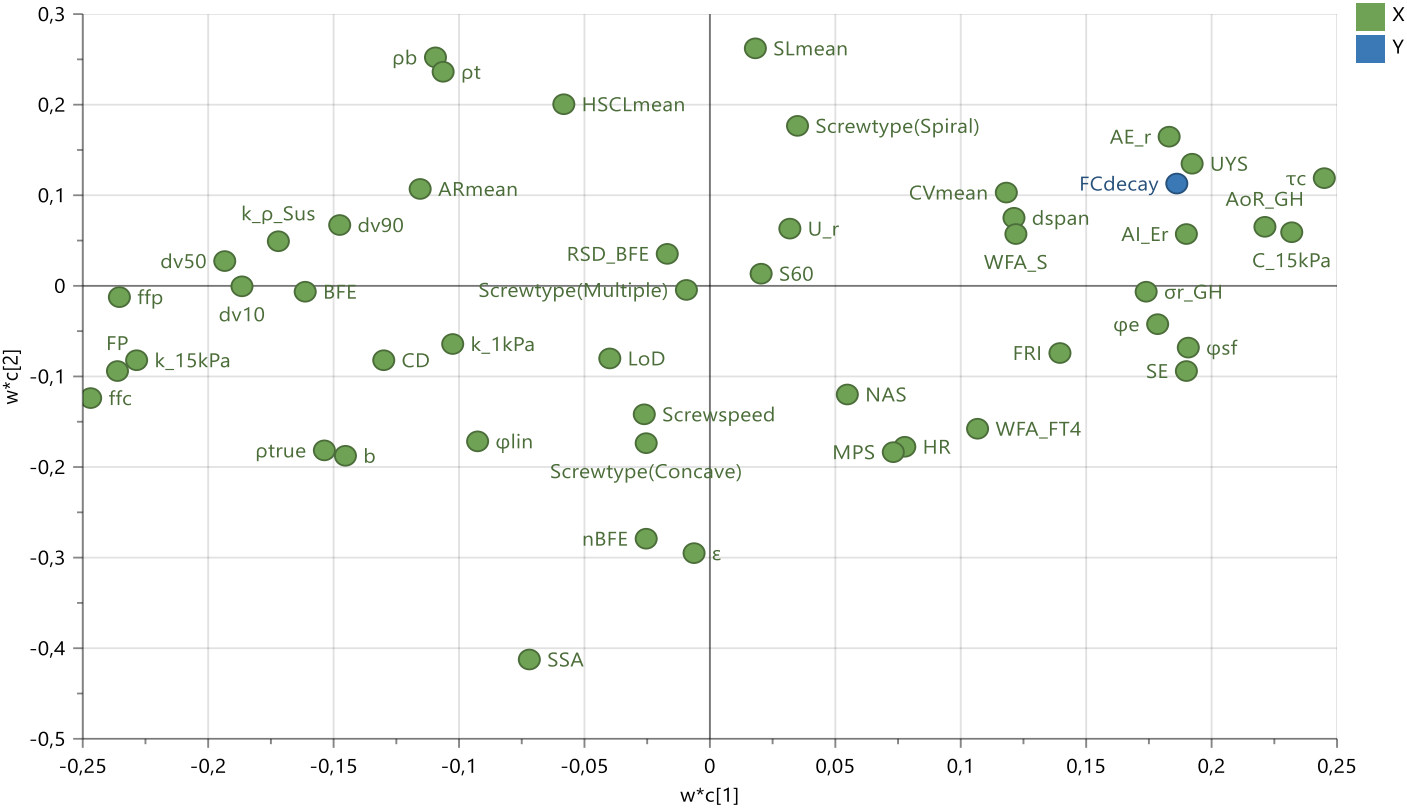


Figure 15: PC 1 vs PC 2 loadings plot of the FC_{decay} model.

Another set of descriptors with a positive correlation to FC_{decay} are AE_r and AI_{Er}, describing the fluidization of a powder bed. A completely fluidized powder bed (i.e. low AE_r) will be able to maintain a constant feed capacity for a longer period of time due to an easier flow in the screw flights. On the other hand, materials with high cohesive or adhesive properties (τ_c, AoR_{GH}, UYS) show difficulties to achieve consistent screw flight filling, explaining their location close to FC_{decay} (**Figure 15**). The negative correlation of flow, density and particle size with FC_{decay} was confirmed by their location on the opposite side of the origin. Consequently, materials like DCP (high density and good flow) and MCL100 (good flow and bigger particles) show a low FC_{decay}.

As screw speed and screw type were located close to the origin, it can be concluded that there was no significant correlation with FC_{decay} . This means that changing the screw type or screw speed, does not significantly affect the hopper fill level at which the feed capacity starts to decrease (**Figure 15**).

The correlations for the volumetric feeding responses described above were also observed by Bostijn et al. (2019) on a low-throughput feeder, demonstrating that the impact of material properties and feeder configuration follow the same trends for both low- and high-throughput feeders.

5.4 Gravimetric feeder trials

5.4.1 Partial least squares regression modeling

The gravimetric feeding responses were included into one overall PLS model with a goodness of fit (R^2Y) and prediction (Q^2) of 67.4% and 58.7%, respectively. An overview of the R^2Y and Q^2 for each response is given in **Table 7**. Similar to the PLS modeling of the volumetric feeder trials, correlations between the material properties, process settings and selected feeder responses (i.e. RSD_{LC} , $STRSD$, V_{refill} and RSD_{refill}) were established. During gravimetric feeding the control system was active, in order to minimize the variability on the mass flow rate. This means that any major deviations (e.g. high RSD_{LC} or high $STRSD$) in the mass flow profile were due to the current controller settings and are not purely related to the material properties or process settings. **Figure 16** shows the scores and loadings plot (PC1 vs. PC2) for the overall PLS model.

Table 7: Overview of the constructed PLS model for the gravimetric feeder trials with the responses.

Overall model			Responses		
R^2Y	Q^2	#PC	Name	R^2Y	Q^2
0.674	0.587	3	RSD_{LC}	0.547	0.414
			$STRSD$	0.471	0.300
			V_{refill}	0.893	0.884
			RSD_{refill}	0.782	0.741

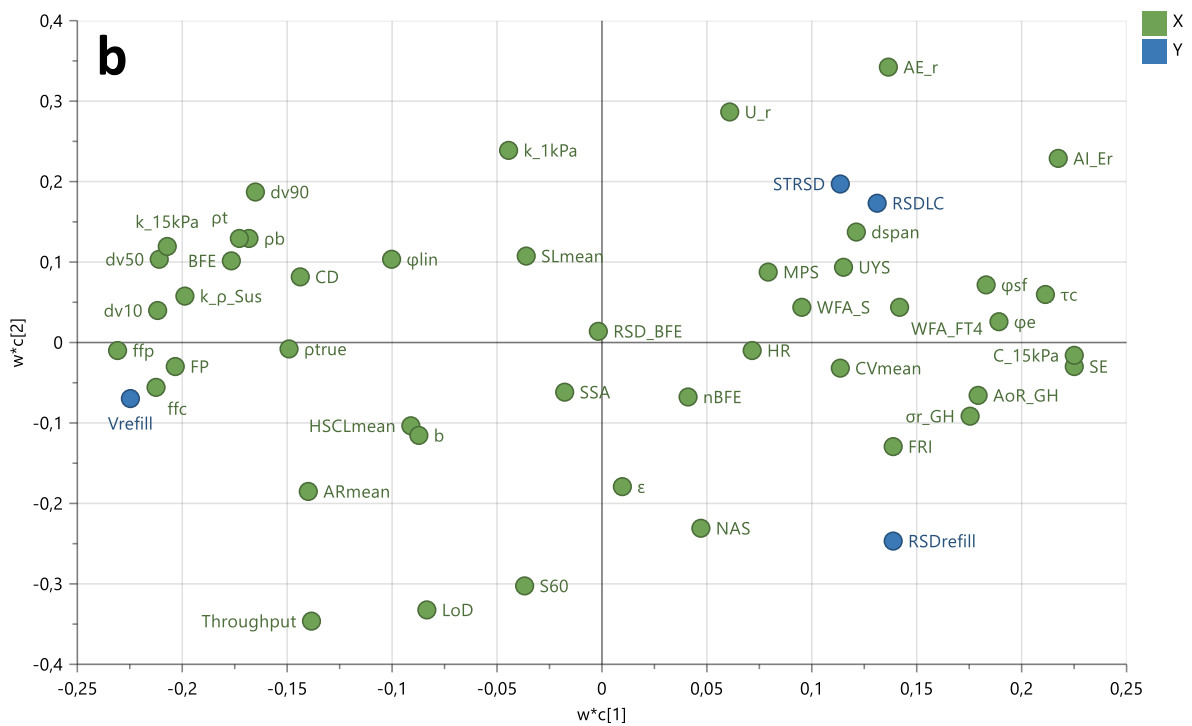
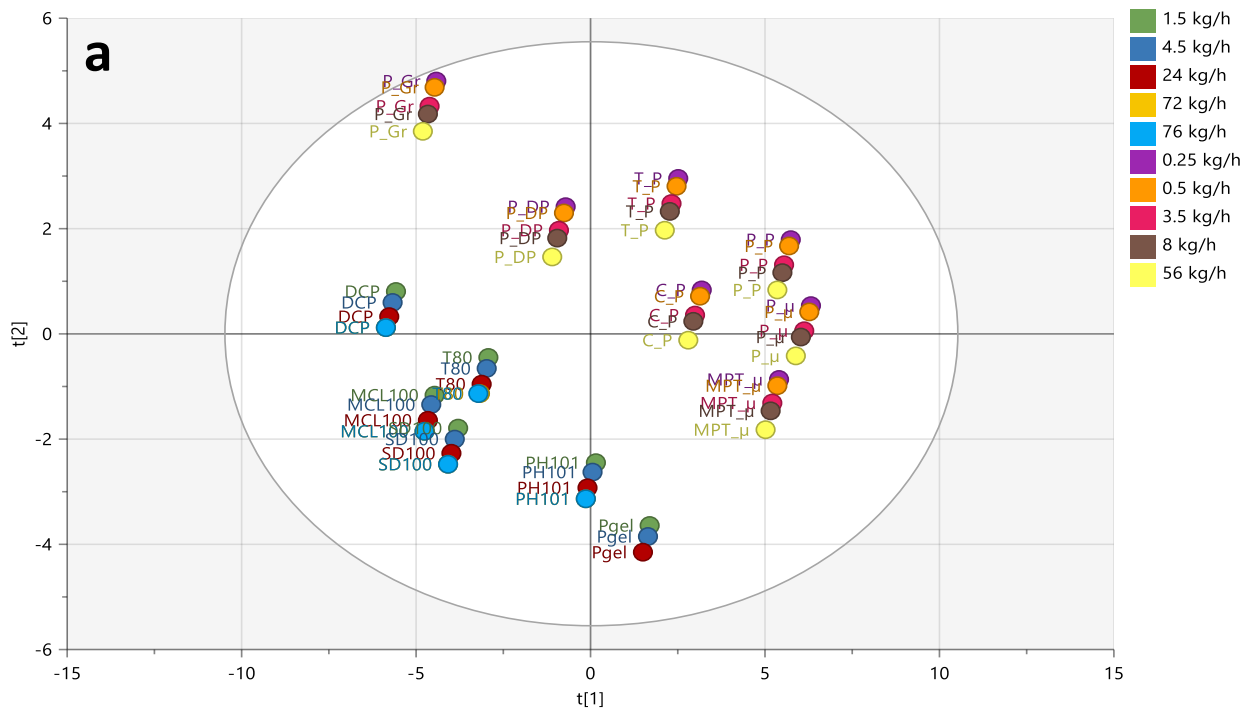


Figure 16: PC 1 vs PC 2 scores (a) and loadings (b) plot of the gravimetric PLS model.

5.4.1.1 Mass flow variability

Both descriptors of mass flow variability during gravimetric feeding were found in the same location on the loadings plot (**Figure 16b**), indicating a strong correlation between both the short-term (STRSD) and long term (RSD_{LC}) variability. As the gravimetric control loop attempts to reduce the variability induced by the material properties and process settings, any remaining variability can be linked to the current control system settings to cope with this variability. Furthermore, a negative correlation was found between the throughput and mass flow variability since these were located at opposite sides from the origin. Consequently, a higher mass flow rate will result in lower mass flow variabilities. The influence of the mass flow rate could be linked to the observations during the volumetric trials where STRSD and RSD_{FCmax} increased exponentially at lower screw speeds (i.e. equal to lower mass flow rates)(**Figure 14**), indicating challenges of feeding at lower throughputs. As previously concluded by Bostijn et al. (2019) and Ervasti et al. (2015), the standard deviation (SD) was similar for both high and low throughput runs, but normalizing this SD by a higher mean mass flow for high throughput runs resulted in the lower RSD_{LC} and STRSD values. Two other descriptors that show a clearly negative correlation are LOD and S60 (**Figure 16b**). This was most likely due to confounding, since most of the materials with poor flow showed a low moisture content.

Similarly as observed for the feed capacity variability during volumetric feeding, poor and inconsistent screw flight filling was the main reason for a high variability in mass flow. This was confirmed by the location of the descriptors (i.e. on the opposite side of the loadings plot) for materials with a good flow (e.g. ffp, BFE, dv50), high permeability (e.g. k_{15kPa} , k_{ρ_Sus}) and high density (ρ_t and ρ_b). Consequently, the descriptors for materials with a high wall friction angle, cohesion, compressibility, angle of repose and incomplete fluidization of the powder bed were clustered close to the mass flow variability responses (**Figure 16b**).

5.4.1.2 Refill consistency

The descriptor V_{refill} is a representation of the amount of material that was added from the top-up system into the hopper of the feeder. Keeping into consideration that the top-up level was regulated via a level sensor, the volume of material added should be the same for each refill. As this was not the case for all materials, it suggests that these issues are related to the raw material properties.

V_{refill} was mainly determined by descriptors comprised in PC1 since V_{refill} is located close to zero along PC2. A clear correlation between V_{refill} and the descriptors for flow (i.e. ffp, ffc and FP), permeability (i.e. k_{15kPa} and k_{ρ_Sus}), compressibility (i.e. C_{15kPa}) and density (e.g. ρ_b , ρ_t) was found. Materials that flow and fluidize well in the system will result in a highly consistent flow of

powder going from their container to the top-up system (i.e. through the dilute-phase pneumatic powder supply) and from the top-up system into the feeder (i.e. via a butterfly valve), thus material loss along the way. Consequently, materials that show a high tendency to stick to surfaces or each other, have incomplete fluidization or have a high compressibility will not achieve a consistent powder flow through the system, possibly resulting in a lower volume of material reaching the feeder. **Figure 17a** shows the formation of a rathole at the inlet of the vacuum conveying lance in the container of PH101. The absence of fresh material at the inlet resulted in a lower volume added into the top-up system (i.e. low V_{refill}), which could introduce extra variability (i.e. higher $\text{RSD}_{\text{refill}}$) during a gravimetric feeder run. A solution for this problem could be using a top-up system based on gravity, keeping in mind that a reduced flowability of materials could also generate problems via this system (i.e. bridge formation).



Figure 17: (a) Rathole formation at the inlet of the vacuum conveying lance in the container of PH101. (b) Sticking and layering of Pharmgel (Pgel) to the conical hopper walls of the top-up system.

The influence of material properties on the refill consistency was also shown by the location of the descriptor $\text{RSD}_{\text{refill}}$. This descriptor was anti-correlated with V_{refill} indicating that the opposite conclusions are valid for this response. Consequently, materials with a high consistent powder flow (e.g. high f_{fc} , high ρ_{b} and ρ_{t} , high $k_{15\text{kPa}}$) will contribute to a lower $\text{RSD}_{\text{refill}}$ value. Additionally, materials that tend to adhere to surfaces or are difficult to fluidize will fail to reach a consistent powder flow (i.e. high $\text{RSD}_{\text{refill}}$ values) (**Figure 16b**). As depicted in **Figure 17b**, sticking of material (e.g. materials that are highly cohesive or adhesive) to the hopper wall can cause a higher variability in the amount of material added to the feeder (i.e. high $\text{RSD}_{\text{refill}}$). Additionally, in extreme cases it is possible that a layer is formed on top of the level sensor, giving a false positive signal. Consequently, no fresh material will be supplied to the top-up system and thus to the feeder (i.e. low V_{refill}). The layering process itself is hard to avoid, but lowering the top-up volume (i.e. physically lowering the sensor position) could limit the sticking behavior through a reduction in powder densification.

5.4.2 Overshoot quantification

During hopper refill the feeder switches to volumetric mode. When this mode is active, the feeding mass flow will be sensitive to density changes caused by a drop of fresh material on top of the material already present material in the hopper. These density changes could result in overshoots in the mass flow profile, as demonstrated in **Figure 18**. To quantify and investigate the consistency of such overshoots during a gravimetric run, the area under the curve (Res_{AUC}), duration (Res_D) and amplitude (Res_A) were calculated using equations 6 and 7.

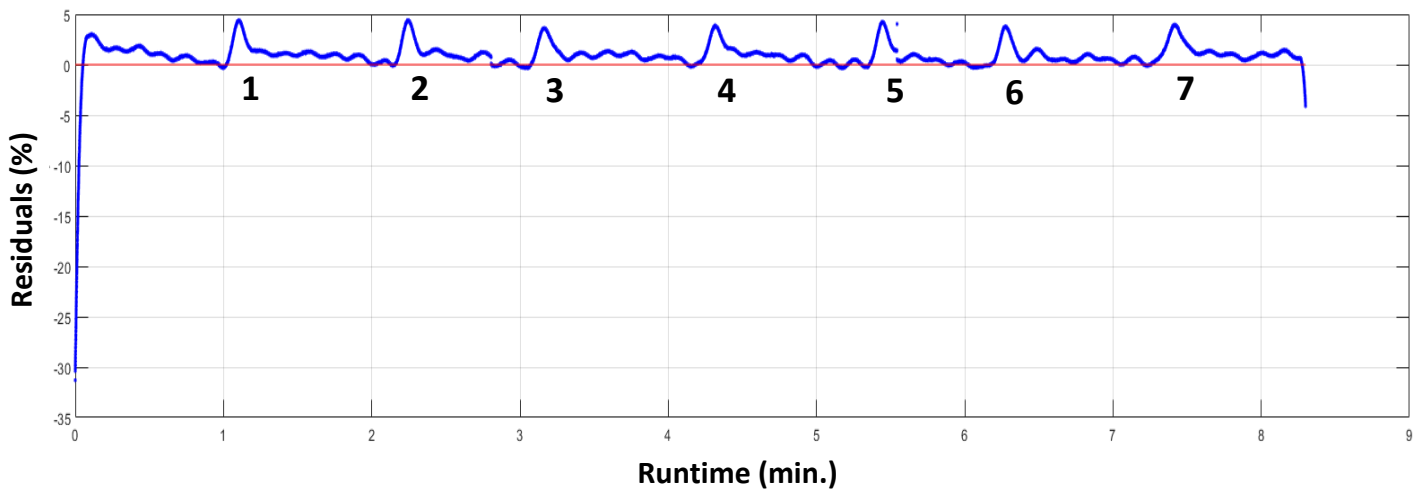


Figure 18: Residual plot of MCL100 at a throughput of 76 kg/h with twin-spiral screws used to demonstrate the overshoots during refills. Each overshoot created during a refill was numbered.

Table 8 gives an overview of the calculated responses for each of the overshoots seen in **Figure 18**. The responses show a high consistency in their value, which was observed for every selected material (not shown). Small differences between the refill overshoots were due to the variability in amount of material that was added by the top-up system. Additionally, each selected raw material showed different degrees of magnitude for the overshoots, suggesting a correlation with their properties (e.g. compressibility) and selected screw type for that specific material. Due to a low goodness of fit (i.e. 17.7%) and prediction (i.e. 5.29%) of the generated PLS models (not shown), no conclusions could be made and further experiments (e.g. longer refill periods, different refill levels, investigating influence of screw type on refill overshoots) are needed. Eventually, the implementation of an optimized control system that could predict these overshoots based on the material properties could be helpful to reduce the deviations (e.g. a material specific optimized refill control algorithm).

Table 8: *ResAUC, ResD and ResA calculated for the overshoots observed during a gravimetric run of MCL100 at 76 kg/h (figure 17).*

#Overshoot	Res _{AUC} (% x min.)	Res _D (s)	Res _A
1	0.4481	12.09	0.0371
2	0.4661	13.31	0.0350
3	0.4539	15.10	0.0301
4	0.5550	18.33	0.0303
5	0.4439	13.55	0.0328
6	0.4865	16.04	0.0303
7	0.5146	15.28	0.0337
Mean	0.4812	14.81	0.0327
RSD (%)	8.506	13.90	8.258

6. Conclusion

In this study, a quantitative relationship between material properties, process settings and screw feeding responses was established via multivariate models (PLS). The developed PLS models elucidated that the material properties and process settings were clearly correlated to the feeding behavior. The often used material properties describing the screw filling potential (i.e. density, flow, fluidization potential, cohesion and particle size) were the main contributors for the responses of both volumetric and gravimetric feeder models. Measuring the compressibility, permeability and wall friction angle provided an alternative method to determine the feeding behavior of a powder. Additionally, the extended volumetric feeder trials pointed out that there was a significant influence of the chosen screw type and screw speed on the feeding process (i.e. FC_{max} and feeding variability). The application of polynomial curve fitting on the mass flow profiles suggested a correlation between the material properties (i.e. compressibility and density) and the magnitude of an overshoot after refill, but requires additional experiments to determine the quantitative relationship. Finally, the feeding process could be optimized by reducing the feeding variability through the application of optimized mass flow filters, high frequency vibrations, independent agitator control and optimized top-up systems. Overall, the developed PLS models could allow the prediction of the feeding performance for a wide range of materials based on the characterization of a subset of material properties. This approach could result in a reduction in the number of feeding experiments needed to optimize a process and increase the speed of development for new drug products.

Acknowledgments

This work was supported by the agency Flanders Innovation and Entrepreneurship (Project n° HBC.2018.0135) and Fette Compacting. Brabender and Fette Compacting Belgium are acknowledged for kindly providing support during the project.

References

- Bostijn N, Dhondt J, Ryckaert A, Szabó E, Dhondt W, Van Snick B, et al. A multivariate approach to predict the volumetric and gravimetric feeding behavior of a low feed rate feeder based on raw material properties. *Int J Pharm* [Internet]. 2019;557(December 2018):342–53. Available from: <https://doi.org/10.1016/j.ijpharm.2018.12.066>
- Brabender Technology, 2020. Information G, Specification M, Modules C, Drawings T. Screw Feeder DDSR20 2.0 (AC-motor);0(3). https://www.brabender-technologie.com/fileadmin/media/Werksnormen/DDSR20/PDF/DDW-M-DDSR20_AC_-E.pdf
- Cartwright, J.J., Robertson, J., D’Haene, D., Burke, M.D., Hennenkamp, J.R., 2013. Twin screw wet granulation: Loss in weight feeding of a poorly flowing active pharmaceutical ingredient. *Powder Technol.* 238, 116–121. <https://doi.org/10.1016/j.powtec.2012.04.034>
- Coperion K-Tron, Smart Feeding Solutions 2012 for Bulk Material Processing.
- Dunst, Paul, et al. "Vibration-Assisted Handling of Dry Fine Powders." *Actuators*, vol. 7, no. 2, 2018, p. NA. Gale Academic OneFile <https://doi.org/10.3390/act7020018>
- Engisch, W.E., Muzzio, F.J., 2012. Method for characterization of loss-in-weight feeder equipment. *Powder Technol.* 228, 395–403. <https://doi.org/10.1016/j.powtec.2012.05.058>
- Engisch WE, Muzzio FJ. Loss-in-Weight Feeding Trials Case Study: Pharmaceutical Formulation. *J Pharm Innov.* 2014;10(1).
- Engisch, W., Muzzio, F., 2015a. Using Residence Time Distributions (RTDs) to Address the Traceability of Raw Materials in Continuous Pharmaceutical Manufacturing. *J. Pharm. Innov.* 11, 64–81. <https://doi.org/10.1007/s12247-015-9238-1>
- Engisch, W.E., Muzzio, F.J., 2015b. Feedrate deviations caused by hopper refill of loss-in-weight feeders. *Powder Technol.* 283, 389–400. <https://doi.org/10.1016/j.powtec.2015.06.001>
- Ervasti T, Simonaho SP, Ketolainen J, Forsberg P, Fransson M, Wikström H, et al. Continuous manufacturing of extended release tablets via powder mixing and direct compression. Vol. 495, *International Journal of Pharmaceutics*. 2015. p. 290–301. <https://doi.org/10.1016/j.ijpharm.2015.08.077>
- Ierapetritou, M., Muzzio, F., Reklaitis, G., 2016. Perspectives on the continuous manufacturing of powder-based pharmaceutical processes. *AIChE J.* 62, 1846–1862. <https://doi.org/10.1002/aic.15210>
- Rogers A, Hashemi A, Ierapetritou M. Modeling of Particulate Processes for the Continuous Manufacture of Solid-Based Pharmaceutical Dosage Forms. *Processes*. 2013;1(2):67–127.
- Simonaho, S.-P., Ketolainen, J., Ervasti, T., Toiviainen, M., Korhonen, O., 2016. Continuous manufacturing of tablets with PROMIS-line - Introduction and case studies from continuous

- feeding, blending and tableting. *Eur. J. Pharm. Sci.*, Volume 90, 2016, Pages 38-46, ISSN 0928-0987
<https://doi.org/10.1016/j.ejps.2016.02.006>
- Van Snick, B., Holman, J., Vanhoorne, V., Kumar, A., De Beer, T., Remon, J.P., Vervaet, C., 2017b. Development of a continuous direct compression platform for low-dose drug products. *Int. J. Pharm.* 529. <https://doi.org/10.1016/j.ijpharm.2017.07.003>
- Van Snick, B., Holman, J., Cunningham, C., Kumar, A., Vercruyse, J., De Beer, T., Remon, J.P., Vervaet, C., 2017a. Continuous direct compression as manufacturing platform for sustained release tablets. *Int. J. Pharm.* 519. <https://doi.org/10.1016/j.ijpharm.2017.01.010>
- Van Snick, B., Dhondt, J., Pandelaere, K., Bertels, J., Mertens, R., Klingeleers, D., Di Pretoro, G., Remon, J.P., Vervaet, C., De Beer, T., Vanhoorne, V., 2018. A multivariate raw material property database to facilitate drug product development and enable in-silico design of pharmaceutical dry powder processes. *Int. J. Pharm.* 549, 415–435.
<https://doi.org/https://doi.org/10.1016/j.ijpharm.2018.08.014>
- Van Snick B, Kumar A, Verstraeten M, Pandelaere K, Dhondt J, Di Pretoro G, et al. Impact of material properties and process variables on the residence time distribution in twin screw feeding equipment. *Int J Pharm.* 2019;556:200–16. <https://doi.org/10.1016/j.ijpharm.2018.11.076>
- Van Snick B. Experimental and model-based analysis of a continuous direct compression platform for oral solid dosage manufacturing. [Ghent, Belgium]: Ghent University. Faculty of Pharmaceutical Sciences; 2019 <http://hdl.handle.net/1854/LU-8610640>